ARTICLE

doi:10.1038/nature16057

# Novel antibody–antibiotic conjugate eliminates intracellular *S. aureus*

Sophie M. Lehar[1], Thomas Pillow[2], Min Xu[3], Leanna Staben[2], Kimberly K. Kajihara[1], Richard Vandlen[4], Laura DePalatis[4], Helga Raab[4], Wouter L. Hazenbos[1], J. Hiroshi Morisaki[1], Janice Kim[3], Summer Park[3], Martine Darwish[4], Byoung-Chul Lee[4], Hilda Hernandez[5], Kelly M. Loyet[5], Patrick Lupardus[6], Rina Fong[6], Donghong Yan[3], Cecile Chalouni[7], Elizabeth Luis[4], Yana Khalfin[5], Emile Plise[8], Jonathan Cheong[8], Joseph P. Lyssikatos[2], Magnus Strandh[9], Klaus Koefoed[9], Peter S. Andersen[9], John A. Flygare[2], Man Wah Tan[1], Eric J. Brown[1] & Sanjeev Mariathasan[1]

***Staphylococcus aureus* is considered to be an extracellular pathogen. However, survival of *S. aureus* within host cells may provide a reservoir relatively protected from antibiotics, thus enabling long-term colonization of the host and explaining clinical failures and relapses after antibiotic therapy. Here we confirm that intracellular reservoirs of *S. aureus* in mice comprise a virulent subset of bacteria that can establish infection even in the presence of vancomycin, and we introduce a novel therapeutic that effectively kills intracellular *S. aureus*. This antibody–antibiotic conjugate consists of an anti-*S. aureus* antibody conjugated to a highly efficacious antibiotic that is activated only after it is released in the proteolytic environment of the phagolysosome. The antibody–antibiotic conjugate is superior to vancomycin for treatment of bacteraemia and provides direct evidence that intracellular *S. aureus* represents an important component of invasive infections.**

*S. aureus* is the leading cause of bacterial infections in humans worldwide and represents a major health problem in both hospital and community settings[1]. However, *S. aureus* is not exclusively a pathogen and commonly colonizes the anterior nares and skin of healthy individuals. When infection does occur, the most serious infections such as endocarditis, osteomyelitis, necrotizing pneumonia and sepsis take hold after dissemination of the bacteria into the bloodstream[2]. Over the last several decades, infection with *S. aureus* has become increasingly difficult to treat due to the emergence and rapid spread of methicillin-resistant *S. aureus* (MRSA), which is resistant to all known β-lactam antibiotics[3]. Alarmingly, reduced susceptibility to vancomycin and resistance to linezolid and daptomycin have already been reported in MRSA clinical strains[4].

Investigations going back at least 50 years have revealed that *S. aureus* is able to invade and survive inside mammalian cells, including the phagocytic cells that are responsible for bacterial clearance[5–11]. *S. aureus* is taken up by host phagocytic cells, primarily neutrophils and macrophages, within minutes after intravenous infection[12]. While the majority of the bacteria are effectively killed by these cells, incomplete clearance of *S. aureus* inside blood-borne phagocytes can allow these infected cells to act as 'Trojan horses' for dissemination of the bacteria away from the initial site of infection. Indeed, patients with normal neutrophil counts may be more prone to disseminated disease than those with reduced neutrophil counts[5,13,14]. Once delivered to the tissues, *S. aureus* can invade various non-phagocytic cell types, and intracellular *S. aureus* in tissues is associated with chronic or recurrent infections including osteomyelitis[15], recurrent rhinosinusitis[16], pulmonary infections[17] and endocarditis[18]. In addition, intracellular *S. aureus* has been shown to undermine innate immune responses and induce subsequent destruction of neutrophils[19,20]. Together, these data suggest that ablating intracellular *S. aureus* is key to clinical success, but until now there has been no way to test this hypothesis directly.

## Intracellular MRSA are protected from antibiotics

To confirm the hypothesis that mammalian cells provide a protective niche for *S. aureus* in the presence of antibiotic therapy, we compared the efficacy of three major antibiotics that are currently used as the standard of care for invasive MRSA infections (vancomycin, daptomycin and linezolid) against extracellular planktonic bacteria versus bacteria sequestered inside murine macrophages (Table 1). All three antibiotics failed to kill a highly virulent community-acquired MRSA strain, USA300, sequestered inside macrophages exposed to clinically achievable concentrations of the antibiotics, consistent with other studies showing that the majority of existing antibiotics are inefficient at killing intracellular *S. aureus* both *in vitro*[21] and *in vivo*[22].

## Intracellular *S. aureus* spreads infection

To compare directly the virulence of intracellular bacteria versus free-living planktonic bacteria and to determine whether the intracellular bacteria are able to establish infection in the presence of vancomycin *in vivo*, mice were infected with equivalent doses of *S. aureus* taken directly from broth culture or bacteria sequestered inside host peritoneal

**Table 1 | Antibiotic minimum inhibitory concentrations for MRSA.**

| Antibiotics | Extracellular MRSA (MIC (μg ml$^{-1}$)) | Intracellular MRSA (MIC (μg ml$^{-1}$)) | Serum $C_{max}$ (μg ml$^{-1}$) |
|---|---|---|---|
| Vancomycin | 1 | >100 | 50 |
| Daptomycin | 4 | >100 | 60 |
| Linezolid | 0.3 | >20 | 20 |
| Rifampicin | 0.004 | 50 | 20 |

Extracellular MIC is the minimum antibiotic dose that prevented growth of MRSA seeded in trypticase soy broth. Intracellular MIC is the minimum dose that prevented survival of MRSA sequestered inside murine macrophages (> indicates continued growth at the highest antibiotic dose tested). Data are summarized from three different experiments. Serum $C_{max}$, the expected serum concentrations for clinically relevant antibiotics[37].

[1]Infectious Diseases Department, Genentech Inc., South San Francisco, California 94080, USA. [2]Medicinal Chemistry Department, Genentech Inc., South San Francisco, California 94080, USA. [3]Translational Immunology Department, Genentech Inc., South San Francisco, California 94080, USA. [4]Protein Chemistry Department, Genentech Inc., South San Francisco, California 94080, USA. [5]Biochemical and Cellular Pharmacology Department, Genentech Inc., South San Francisco, California 94080, USA. [6]Structural Biology Department, Genentech Inc., South San Francisco, California 94080, USA. [7]Pathology Department, Genentech Inc., South San Francisco, California 94080, USA. [8]Drug metabolism and Pharmacokinetics Department, Genentech Inc., South San Francisco, California 94080, USA. [9]Symphogen A/S, Pederstrupvej 93, DK-2750 Ballerup, Denmark.

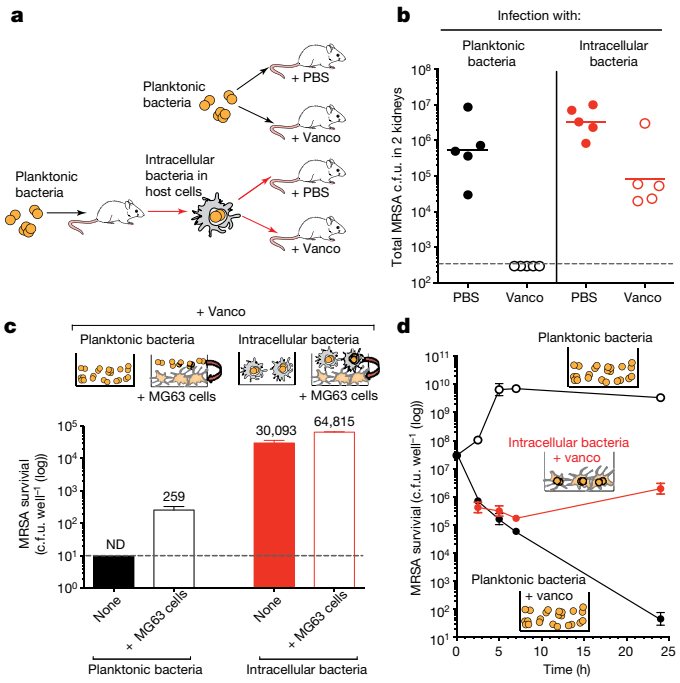


**Figure 1 | Intracellular MRSA are protected from vancomycin.** **a**, Experimental design for generating planktonic versus intracellular bacteria for infection and treatment with vancomycin (vanco). **b**, Bacterial loads in kidney, 4 days after infection. c.f.u., colony-forming units. Each point represents data from a single mouse ($n = 5$ mice per group). **c**, Planktonic or intracellular bacteria were suspended in media containing vancomycin and cultured alone or on a monolayer of MG63, and surviving bacteria were enumerated 1 day later. Error bars represent means ± standard deviation (s.d.). **d**, Survival of MRSA cultured with vancomycin with or without MG63 cells. Error bars show s.d. ND, none detected. Dashed lines indicate the limit of detection. Representative of three independent experiments.

macrophages and neutrophils (Fig. 1a). Mice infected with intracellular bacteria had equivalent or higher bacterial burdens in the kidneys 4 days after infection compared with those infected with planktonic bacteria (Fig. 1b). Infection with intracellular bacteria also resulted in more consistent colonization of the brain (Extended Data Fig. 1). To characterize this observation further, we infected MG63 osteoblasts with either planktonic MRSA or an equivalent number of intracellular MRSA, in the presence of vancomycin. Planktonic bacteria exposed to vancomycin alone were efficiently killed, (Fig. 1c). However, we recovered a small number of surviving bacteria (approximately 0.06% of input) associated with the MG63 cells 1 day after infection, which had been protected from vancomycin by invasion into osteoblasts. MRSA that were sequestered inside peritoneal cells showed a significant increase in both survival and efficiency of MG63 infection in the presence of vancomycin. About 15% of intracellular MRSA in the leukocytes survived under vancomycin exposure identical to that which sterilized cultures of planktonic bacteria. Intracellular *S. aureus* that were sequestered in MG63 cells (Fig. 1d), primary human brain endothelial cells and A549 bronchial epithelial cells (Extended Data Fig. 2) were also able to increase by almost tenfold over a 24 h period under constant exposure to a concentration of vancomycin that killed free-living bacteria. Together, these data suggest that intracellular reservoirs of MRSA in myeloid cells can promote dissemination of infection to new sites in the presence of active antibiotic treatment, and that intracellular growth can occur in a variety of cell types despite constant antibiotic therapy.

## Designing the antibody–antibiotic conjugate

These findings suggested that therapies aimed at eliminating intracellular bacteria may improve clinical success. To test this conclusively, we developed a novel therapeutic that is activated specifically inside mammalian cells that have taken up *S. aureus*. The antibody–antibiotic conjugate (AAC) consists of an anti-*S. aureus* antibody (THIOMAB, engineered to contain unpaired cysteines) covalently linked via the introduced cysteines to a highly efficacious antibiotic using a cathepsin-cleavable linker containing a novel quaternary ammonium salt (Fig. 2a). The resulting AAC has no direct antibacterial activity when bound to planktonic *S. aureus* and does not diffuse into mammalian cells, owing to the size of the antibody. However, when AAC-opsonized bacteria are taken up by host cells, intracellular proteases cleave the linker and readily release the antibiotic in its active form[23] (Fig. 2b). Depending on the antibody specificity, we found that thousands of AACs can bind to a single bacterium and deliver a sufficient concentration of free antibiotic within the phagosome to result in bacterial killing.

The antibody and antibiotic components were carefully chosen and optimized for maximal efficacy. A panel of more than 40 anti-*S. aureus* antibodies were cloned and purified from B cells derived from the peripheral blood of patients recovering from various *S. aureus* infections and screened for binding to a panel of clinically relevant *S. aureus* strains and to USA300 isolated directly *ex vivo* from the kidneys of infected mice. We found the greatest extent of binding with antibodies directed against wall-teichoic acids (WTAs), pathogen-specific polyanionic glycopolymers that are connected to the thick peptidoglycan layers of Gram-positive bacteria (Fig. 2c). *S. aureus* produces WTAs composed of phospho-ribitol repeating units that are further modified by either α- or β-*O*-linked *N*-acetylglucosamine (GlcNAc) sugars mediated by TarM or TarS glycosyltransferases, respectively[24]. A human immunoglobulin $G_1$ ($IgG_1$) that recognizes β-*O*-linked GlcNAc sugar modifications on WTA bound to all *S. aureus* strains tested. Monoclonal antibodies recognizing the α-*O*-linked GlcNAc bound well to *S. aureus* strains cultured *in vitro*; however, expression of the α-*O*-linked GlcNAc was absent on some *S. aureus* isolates. On those strains that co-expressed the α- and β-*O*-linked GlcNac, β-specific antibodies yielded consistently higher binding to *in vivo*-derived MRSA (Fig. 2c). Antigen specificity of the antibodies was confirmed by genetic means, such that antibodies against α- or β-GlcNAc sugar modifications on WTAs failed to bind to *S. aureus* strains lacking the TarM or TarS glycosyltranferase, respectively (Fig. 2d). We estimate that ~15,000 β-WTA-specific antibodies can bind to protein-A-deficient *S. aureus* USA300 by measuring binding of radiolabelled antibodies (data not shown).

To characterize antibody binding to WTA at the molecular level further, we co-crystallized the Fab fragment from an anti-β-WTA antibody in complex with a synthetic form of the minimal repeating β-WTA unit (C2 carbon of ribitol-1-phosphate linked to the C1 position in GlcNAc via a β-glycosidic bond) and determined a crystal structure of the complex at 1.7 Å resolution (Extended Data Table 1). The structure reveals how the minimal β-WTA epitope binds to the complementarity determining region (CDR) of the Fab antibody fragment (Fig. 2e). The heavy chain H1 and H3 CDR loops form a binding site for the GlcNAc, with the GlcNAc hexose ring stacking against the Trp 33 indole side chain. Importantly, the antibody has an extended L1 loop containing two arginine residues (Arg 27d and 28) that interact with the phosphate group on the ribitol backbone. This arginine 'tweezers' motif triangulates the ribitol phosphodiester backbone in relation to the GlcNAc moiety, and is probably a key reason for the β-anomer-specific recognition of GlcNAc-WTA by the antibody.

An extensive set of criteria was used to choose the optimal antibiotic for the AAC platform. We chose the rifamycin class of antibiotics for their high potency, unaltered bactericidal activity in low phagolysosomal pH, and their ability to withstand intracellular insults. A rifamycin derivative (a rifalogue) that allowed connection to the linker antibody through a tertiary amine (T. Pillow, manuscript in preparation) had optimum physicochemical properties to allow for efficient bacterial killing. The chemical groups known to make direct contact with

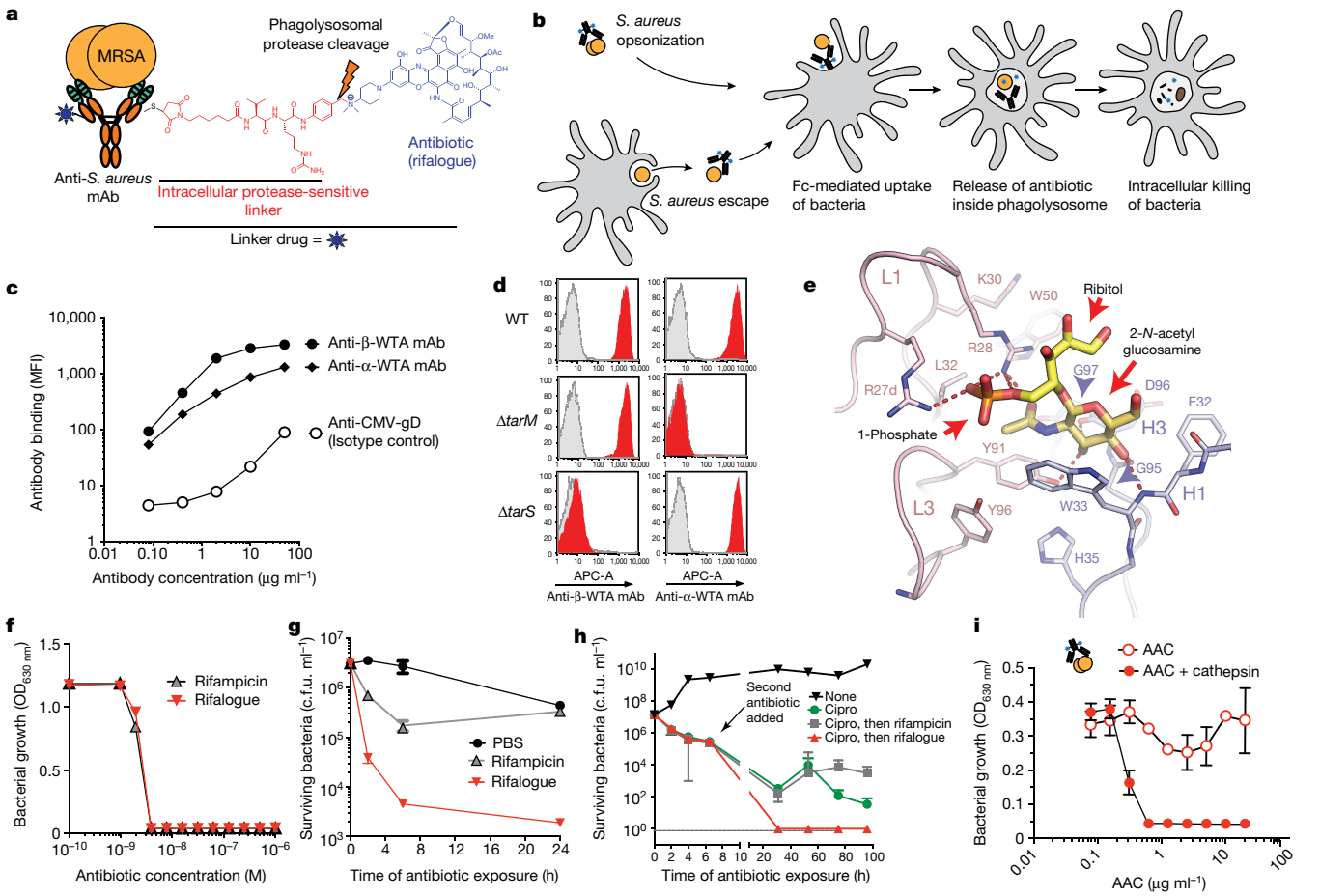


**Figure 2 | AAC design. a**, Model of AAC (not drawn to scale). **b**, Mechanism of AAC action. **c**, Binding of Alexa-488 anti-β-GlcNAC WTA monoclonal antibody (mAb) or anti-α-GlcNAC WTA monoclonal antibody, or isotype control antibody, anti-cytomegalovirus glycoprotein-D (gD) to USA300 isolated from infected kidneys ($n = 3$). MFI, mean fluorescence intensity. **d**, Binding of anti-GlcNAC WTA antibodies (red) or isotype control (grey) to protein-A-deficient USA300 lacking *tarM* or *tarS* ($n = 3$). WT, wild type. **e**, Crystal structure of anti-β-GlcNAc WTA Fab bound to a synthetic minimal β-WTA unit. Antibody light chain (pink) and heavy chain (blue) are shown. **f**, MIC determination for rifampicin and rifalogue on USA300 ($n = 5$). **g**, Survival of stationary phase USA300 incubated with $1 \times 10^{-6}$ M rifampicin or rifalogue ($n = 4$). **h**, USA300 bacteria were incubated without antibiotic (black) or with 3 μg ml$^{-1}$ ciprofloxacin (Cipro; green, red and grey). 1 μg ml$^{-1}$ of rifalogue (red) or rifampicin (grey) was added as indicated ($n = 3$). **i**, Intact AAC does not kill planktonic bacteria but does after pre-treatment with cathepsin-B ($n = 3$). **g**–**i**, Error bars show s.d. for triplicate samples ($n =$ biological repeats).

bacterial RNA polymerase are conserved between rifampicin and the rifalogue[25]. Consistent with this, the minimum inhibitory concentration (MIC) for the rifalogue is identical to rifampicin ($4 \times 10^{-9}$ M), as measured in a conventional growth inhibition assay using planktonic bacteria (Fig. 2f). The rifalogue, but not rifampicin, resulted in a more than 1,000-fold decrease in the number of viable, but non-replicating, bacteria after overnight incubation in minimal PBS buffer (Fig. 2g). The rifalogue was also able to kill classically defined persister cells, bacteria that presumably enter a dormant state to survive antibiotic treatment (for example, ciprofloxacin) of growing cultures[26] (Fig. 2h), while treatment with rifampicin had no effect on recovery of persister cells, in agreement with previous observations[26]. Additionally, rifalogue, but not rifampicin, was able to kill non-dividing MRSA sequestered inside murine macrophages, in part due to its capacity to accumulate rapidly in mammalian cells (Extended Data Fig. 3). As predicted, the rifalogue had no ability to kill extracellular bacteria when linked to the anti-β-WTA monoclonal antibody in the AAC format, but was fully bactericidal after the AAC was treated with cathepsin B to release the active antibiotic (Fig. 2i).

To confirm that the linker used in the AAC is cleaved after internalization of the AAC inside cells, we examined cleavage of the linker with a fluorescence resonance energy transfer (FRET)-based probe consisting of the same anti-MRSA antibody conjugated to two dye molecules that were separated by the same linker used in the AAC[27]. When the fluorescent molecules are covalently associated, fluorescence at 488 nm is quenched; upon cleavage of the linker, quenching is lost. Video microscopy demonstrated that the linker was cleaved within minutes of uptake of the MRSA opsonized with the FRET conjugate (Fig. 3a). We confirmed by mass spectrometry analysis that free rifalogue was released inside macrophages after uptake of MRSA opsonized with active AACs, but not when opsonized with a non-cleavable version of the AAC, which was prepared by replacement of the natural amino acid L-citrulline with D-citrulline at the P1 position, making the linker uncleavable by cathepsins (Fig. 3b).

## AACs eradicate intracellular *S. aureus* infections

When the AAC was used to opsonize MRSA, it readily killed bacteria inside the macrophages, whereas the same bacteria opsonized with non-cleavable β-WTA AAC or monoclonal antibody alone survived (Fig. 3c). AAC-opsonized MRSA were killed inside every cell type tested, including human macrophages, endothelial and epithelial cell lines (Fig. 3d). These data demonstrate that the AAC releases active antibiotic and kills *S. aureus* only after internalization inside host cells, providing a unique tool to assess the importance of intracellular *S. aureus* in various settings. To determine whether specifically targeting intracellular *S. aureus* could prevent cell-to-cell transfer of bacteria, infected peritoneal cells were incubated with MG63 osteoblast cells in the presence of vancomycin (Fig. 3e). Addition of AAC to the

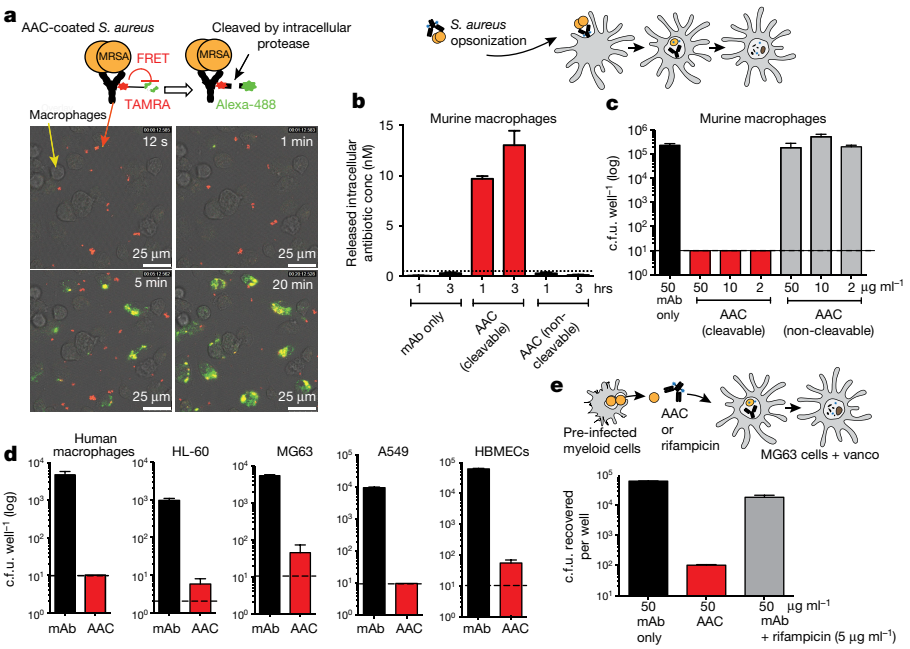


**Figure 3 | AAC linker is cleaved after internalization of bacteria.** **a**, Live cell imaging monitoring cleavage of AAC linker in macrophages with FRET-based antibody conjugate (representative of three fields). TAMRA, tetramethylrhodamine. **b**, Mass spectrometric quantification of released antibiotic inside macrophages from AAC made with standard (cleavable) or non-cleavable linker. mAb, monoclonal antibody. **c**, **d**, USA300, opsonized with antibody, AAC, or non-cleavable AAC, enumerated 48 h after incubation with indicated cells lines. HBMECs, human brain microvascular endothelial cells. Horizontal line indicates the limit of detection. **e**, Intracellular USA300 as in Fig. 1a were added to a monolayer of MG63 with antibody, AAC, or a mixture of antibody plus rifampicin in media containing vancomycin (vanco). Surviving bacteria were enumerated 24 h later. **b**–**e**, Error bars represent means ± s.d. from triplicate wells. Data are representative of 2–4 biological replicates.

culture media resulted in a significant reduction in the number of viable intracellular bacteria recovered 1 day after infection. Similar treatment with the unconjugated anti-MRSA antibody plus a tenfold higher molar concentration of rifampicin, purported to be one of the best-known antibiotics for treatment of intracellular bacteria[28], had very marginal efficacy. To confirm that targeting intracellular *S. aureus* could also prevent transfer of infection from intracellular reservoirs *in vivo*, mice were infected by intravenous injection with equivalent doses of planktonic or intracellular MRSA and then treated with PBS or vancomycin, with or without a single dose of AAC. In the presence of vancomycin only intracellular bacteria were able to efficiently colonize the brain (Extended Data Fig. 1); however, treatment with a single dose of AAC effectively eliminated the bacteria that had escaped vancomycin treatment (Extended Data Fig. 4)

## AAC is superior to vancomycin *in vivo*

To determine the role of intracellular infection in bacteraemia, AACs were tested in an intravenous infection model. First, we tested the efficacy of unconjugated anti-MRSA antibodies by treating mice with either anti-β-WTA antibodies, anti-α-WTA antibodies or intravenous immunoglobulin (IGIV), a pooled immunoglobulin preparation from ~10,000 humans, 1 h before intravenous infection with wild-type USA300 MRSA. *S. aureus* is a common colonizer of human skin and mucosal surfaces and preliminary analysis of multiple sources of human serum, including IGIV, demonstrated that human serum contains approximately 300 µg ml$^{-1}$ of anti-*S. aureus* antibodies, of which ~70% are directed towards the GlcNAc modifications of WTA (Extended Data Fig. 5). Even in this prophylactic treatment setting, unconjugated antibodies did not have any efficacy in preventing infection, whereas treatment with vancomycin eliminated detectable bacteria (Fig. 4a). However, the efficacy of vancomycin was limited when treatment was initiated several hours after infection was established (Fig. 4b). In at least one model of bacteraemia, 95% of the bacteria in blood are found to be associated with neutrophils within 15 min (ref. 6), suggesting that failure of vancomycin in this model could be due to antibiotic escape through survival inside host cells. To test this directly, mice were treated with a single dose of AAC 24 h after infection. A single dose of AAC was efficacious and proved superior to twice daily vancomycin treatment initiated at the same time (Fig. 4c and Extended Data Fig. 6a).

Mouse serum has no appreciable anti-*S. aureus* antibody. To determine whether endogenous anti-WTA antibodies found in normal human serum might compete for binding with the AAC, SCID mice were reconstituted with physiological levels of human IgG by daily treatment with IGIV. The resulting SCID-huIgG mice had sustained levels of at least 10 mg ml$^{-1}$ of human IgG in the serum and were equally susceptible to infection with MRSA compared to untreated controls (data not shown). Despite the presence of potentially competing antibodies, a single dose of anti-MRSA AAC administered at 24 h after infection with MRSA was still more efficacious than vancomycin (Fig. 4d). An AAC made with an irrelevant antibody (anti-cytomegalovirus glycoprotein D antibody)—which could still bind to protein A on MRSA—had much less efficacy. AACs made with anti-β-GlcNAc WTA antibodies appeared to be more efficacious than those made with anti-α-GlcNAc WTA antibodies (Extended Data Fig. 6b), suggesting that the extent of antibody binding determines antibiotic delivery. Treatment with the AAC was more effective than treatment with an equivalent dose or repeated dosing of unconjugated rifalogue, and release of the antibiotic from the AAC was essential for efficacy, as an AAC generated with the non-cleavable linker was not efficacious *in vivo* (Fig. 4e).

## Discussion

Treatment of patients with invasive MRSA infections with conventional antibiotics results in failure rates of up to 50% (refs 29–32), in most cases without measurable outgrowth of antibiotic-resistant strains. Survival of antibiotic-susceptible subpopulations of *S. aureus* in the presence of antibiotic treatment is well documented and is probably due to multiple factors, including survival of persister bacteria that are not actively dividing and poor antibiotic exposure of

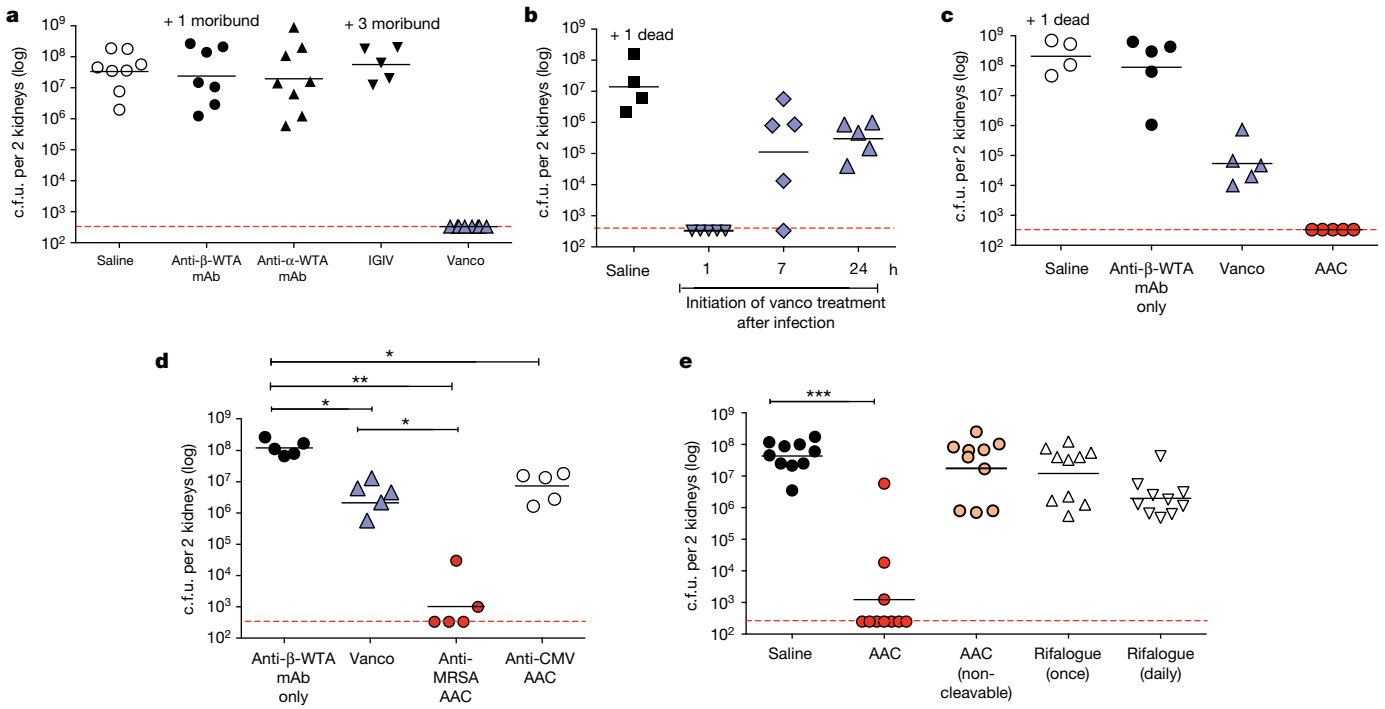


**Figure 4 | AAC is a more effective treatment than vancomycin after intravenous infection. a**, Wild-type (WT) mice ($n = 8$ per group) were treated with 50 mg kg$^{-1}$ of the indicated anti-MRSA antibodies 1 h before MRSA infection or twice daily with 110 mg kg$^{-1}$ vancomycin (Vanco). **b**, Treatment of wild-type mice ($n = 5$ per group) with 110 mg kg$^{-1}$ vancomycin (twice daily) was initiated either at 1 h, 7 h or 24 h after infection. **c**, Wild-type mice ($n = 5$ per group) were treated with saline, anti-β-WTA antibody used in the AAC (monoclonal antibody (mAb)), vancomycin (twice daily), or anti-MRSA AAC (a single dose of 50 mg kg$^{-1}$) starting 24 h after infection. **d**, **e**, SCID mice (**d**, 5 mice per group; **e**, 10 mice per group) were injected with human IgG to achieve a concentration of 10 mg ml$^{-1}$, then infected with MRSA. Treatment as indicated was begun 24 h after infection. Vancomycin, 110 mg kg$^{-1}$ twice daily; AAC, 50 mg kg$^{-1}$ a single dose on day 1; rifalogue, 0.5 mg kg$^{-1}$ either once on day 1, or once daily (days 1–3). **a**–**e**, Bacteria in kidneys were determined 4 days after infection. Schematic of each experimental design is shown in Extended Data Fig. 7. Each point shows data from a single animal. Bars show geometric mean. Dashed lines indicate limit of detection. Mann–Whitney *U*-test. $*P < 0.05$; $**P < 0.01$; $***P < 0.005$.

bacteria in protected niches[33–35]. However, it has been difficult to determine conclusively what role intracellular *S. aureus* plays in disease pathogenesis and antibiotic failure. To address directly the extent to which this ability to survive and replicate inside cells contributes to the failure of conventional antibiotics, we developed a novel therapeutic in the form of an AAC that is specifically designed to be activated only within host cells. We found that a single dose of AAC treatment is effective in a murine model of bacteraemia, in which vancomycin, the current standard of care for MRSA infection, failed (Fig. 4). This suggests that ablation of the intracellular pool of pathogens is key for clinical success in the treatment of potential fatal MRSA infection.

In designing the AAC to test this hypothesis, we used an antibiotic that kills intracellular bacteria. This rifalogue antibiotic also ablates non-replicating bacteria, and antibiotic-resistant persister cells. We posit that this characteristic, along with its ability to accumulate within the intracellular milieu, is essential for AAC success. When the closely related rifampicin, which does not have these characteristics, was conjugated to the same anti-WTA antibody it did not kill intracellular bacteria and exhibited poor efficacy *in vivo* (Extended Data Fig. 8). These studies show that arming antibodies with unique bactericidal antibiotics can result in promising new therapies. Many potent antibiotic-like compounds with the desired characteristics to kill difficult-to-treat intracellular pathogens fail in clinical practice owing to poor pharmacokinetic properties or undesired host toxicity. The use of an AAC might be able to overcome these problems, making it a novel platform for delivering potent antibacterial compounds that may not have a suitable profile as unconjugated drugs. Antibiotic failure has been associated with the ability of a variety of bacterial pathogens to survive within host phagocytic cells[36]. The extent to which other common human pathogens beyond *S. aureus* depend on this intracellular protected niche merits investigation; the AAC platform promises to enhance antibiotic efficacy against these infectious diseases.

**Online Content** Methods, along with any additional Extended Data display items and Source Data, are available in the online version of the paper; references unique to these sections appear only in the online paper.

**Received 15 December 2014; accepted 6 October 2015.**
**Published online 4 November 2015.**

1. Diekema, D. J. *et al.* Survey of infections due to *Staphylococcus* species: frequency of occurrence and antimicrobial susceptibility of isolates collected in the United States, Canada, Latin America, Europe, and the Western Pacific region for the SENTRY Antimicrobial Surveillance Program, 1997–1999. *Clin. Infect. Dis.* **32** (suppl. 2), S114–S132 (2001).
2. Lowy, F. D. *Staphylococcus aureus* infections. *N. Engl. J. Med.* **339,** 520–532 (1998).
3. Boucher, H. W. *et al.* Bad bugs, no drugs: no ESKAPE! An update from the Infectious Diseases Society of America. *Clin. Infect. Dis.* **48,** 1–12 (2009).
4. Nannini, E., Murray, B. E. & Arias, C. A. Resistance or decreased susceptibility to glycopeptides, daptomycin, and linezolid in methicillin-resistant *Staphylococcus aureus*. *Curr. Opin. Pharmacol.* **10,** 516–521 (2010).
5. Thwaites, G. E. & Gant, V. Are bloodstream leukocytes Trojan Horses for the metastasis of *Staphylococcus aureus*? *Nature Rev. Microbiol.* **9,** 215–222 (2011).
6. Rogers, D. E. & Tompsett, R. The survival of staphylococci within human leukocytes. *J. Exp. Med.* **95,** 209–230 (1952).
7. Gresham, H. D. *et al.* Survival of *Staphylococcus aureus* inside neutrophils contributes to infection. *J. Immunol.* **164,** 3713–3722 (2000).
8. Kapral, F. A. & Shayegani, M. G. Intracellular survival of staphylococci. *J. Exp. Med.* **110,** 123–138 (1959).
9. Anwar, S., Prince, L. R., Foster, S. J., Whyte, M. K. & Sabroe, I. The rise and rise of *Staphylococcus aureus*: laughing in the face of granulocytes. *Clin. Exp. Immunol.* **157,** 216–224 (2009).
10. Fraunholz, M. & Sinha, B. Intracellular *Staphylococcus aureus*: live-in and let die. *Front. Cell. Infect. Microbiol.* **2,** 43 (2012).

11. Garzoni, C. & Kelley, W. L. Return of the Trojan horse: intracellular phenotype switching and immune evasion by *Staphylococcus aureus*. *EMBO Mol. Med.* **3,** 115–117 (2011).
12. Rogers, D. E. Studies on bacteriemia. I. Mechanisms relating to the persistence of bacteriemia in rabbits following the intravenous injection of staphylococci. *J. Exp. Med.* **103,** 713–742 (1956).
13. Velasco, E. *et al.* Comparative study of clinical characteristics of neutropenic and non-neutropenic adult cancer patients with bloodstream infections. *Eur. J. Clin. Microbiol. Infect. Dis.* **25,** 1–7 (2006).
14. Venditti, M. *et al. Staphylococcus aureus* bacteremia in patients with hematologic malignancies: a retrospective case-control study. *Haematologica* **88,** 923–930 (2003).
15. Bosse, M. J., Gruber, H. E. & Ramp, W. K. Internalization of bacteria by osteoblasts in a patient with recurrent, long-term osteomyelitis. A case report. *J. Bone Joint Surg. Am.* **87,** 1343–1347 (2005).
16. Clement, S. *et al.* Evidence of an intracellular reservoir in the nasal mucosa of patients with recurrent *Staphylococcus aureus* rhinosinusitis. *J. Infect. Dis.* **192,** 1023–1028 (2005).
17. Jarry, T. M., Memmi, G. & Cheung, A. L. The expression of α-haemolysin is required for *Staphylococcus aureus* phagosomal escape after internalization in CFT-1 cells. *Cell. Microbiol.* **10,** 1801–1814 (2008).
18. Que, Y. A. *et al.* Fibrinogen and fibronectin binding cooperate for valve infection and invasion in *Staphylococcus aureus* experimental endocarditis. *J. Exp. Med.* **201,** 1627–1635 (2005).
19. Greenlee-Wacker, M. C. *et al.* Phagocytosis of *Staphylococcus aureus* by human neutrophils prevents macrophage efferocytosis and induces programmed necrosis. *J. Immunol.* **192,** 4709–4717 (2014).
20. Kobayashi, S. D. *et al.* Rapid neutrophil destruction following phagocytosis of *Staphylococcus aureus*. *J. Innate Immun.* **2,** 560–575 (2010).
21. Barcia-Macay, M., Seral, C., Mingeot-Leclercq, M. P., Tulkens, P. M. & Van Bambeke, F. Pharmacodynamic evaluation of the intracellular activities of antibiotics against *Staphylococcus aureus* in a model of THP-1 macrophages. *Antimicrob. Agents Chemother.* **50,** 841–851 (2006).
22. Sandberg, A., Hessler, J. H., Skov, R. L., Blom, J. & Frimodt-Møller, N. Intracellular activity of antibiotics against *Staphylococcus aureus* in a mouse peritonitis model. *Antimicrob. Agents Chemother.* **53,** 1874–1883 (2009).
23. Dubowchik, G. M. *et al.* Cathepsin B-labile dipeptide linkers for lysosomal release of doxorubicin from internalizing immunoconjugates: model studies of enzymatic drug release and antigen-specific *in vitro* anticancer activity. *Bioconjug. Chem.* **13,** 855–869 (2002).
24. Winstel, V., Xia, G. & Peschel, A. Pathways and roles of wall teichoic acid glycosylation in *Staphylococcus aureus*. *Int. J. Med. Microbiol.* **304,** 215–221 (2014).
25. Campbell, E. A. *et al.* Structural mechanism for rifampicin inhibition of bacterial RNA polymerase. *Cell* **104,** 901–912 (2001).
26. Conlon, B. P. *et al.* Activated ClpP kills persisters and eradicates a chronic biofilm infection. *Nature* **503,** 365–370 (2013).
27. Fischer, R., Hufnagel, H. & Brock, R. A doubly labeled penetratin analogue as a ratiometric sensor for intracellular proteolytic stability. *Bioconjug. Chem.* **21,** 64–73 (2010).
28. Nielsen, S. L. & Black, F. T. Extracellular and intracellular killing in neutrophil granulocytes of *Staphylococcus aureus* with rifampicin in combination with dicloxacillin or fusidic acid. *J. Antimicrob. Chemother.* **43,** 407–410 (1999).
29. Kullar, R., Davis, S. L., Levine, D. P. & Rybak, M. J. Impact of vancomycin exposure on outcomes in patients with methicillin-resistant *Staphylococcus aureus* bacteremia: support for consensus guidelines suggested targets. *Clin. Infect. Dis.* **52,** 975–981 (2011).
30. Fowler, V. G. Jr *et al.* Daptomycin versus standard therapy for bacteremia and endocarditis caused by *Staphylococcus aureus*. *N. Engl. J. Med.* **355,** 653–665 (2006).
31. Yoon, Y. K., Kim, J. Y., Park, D. W., Sohn, J. W. & Kim, M. J. Predictors of persistent methicillin-resistant *Staphylococcus aureus* bacteraemia in patients treated with vancomycin. *J. Antimicrob. Chemother.* **65,** 1015–1018 (2010).
32. Johnson, L. B., Almoujahed, M. O., Ilg, K., Maolood, L. & Khatib, R. *Staphylococcus aureus* bacteremia: compliance with standard treatment, long-term outcome and predictors of relapse. *Scand. J. Infect. Dis.* **35,** 782–789 (2003).
33. Levin, B. R. Noninherited resistance to antibiotics. *Science* **305,** 1578–1579 (2004).
34. Grant, S. S., Kaufmann, B. B., Chand, N. S., Haseley, N. & Hung, D. T. Eradication of bacterial persisters with antibiotic-generated hydroxyl radicals. *Proc. Natl Acad. Sci. USA* **109,** 12147–12152 (2012).
35. Lewis, K. Persister cells. *Annu. Rev. Microbiol.* **64,** 357–372 (2010).
36. Kaiser, P. *et al.* Cecum lymph node dendritic cells harbor slow-growing bacteria phenotypically tolerant to antibiotic treatment. *PLoS Biol.* **12,** e1001793 (2014).
37. Bryskier, A. Anti-MRSA agents: under investigation, in the exploratory phase and clinically available. *Expert Rev. Anti Infect. Ther.* **3,** 505–553 (2005).


**Acknowledgements** This research used resources of the Advanced Photon Source, a US Department of Energy (DOE) Office of Science User Facility operated for the DOE Office of Science by Argonne National Laboratory under contract no. DE-AC02-06CH11357.

**Author Contributions** S.M.L. designed and executed the *in vitro* and *in vivo* analysis of the AAC mechanism of action. T.P., L.S. and J.A.F. designed and synthesized antibiotics and linker drugs. M.X., J.K., S.P. and D.Y. designed and analysed *in vivo* models for intravenous infection. H.R., L.D., M.D. and R.V. designed and conjugated linker antibiotic to antibodies. K.K.K., W.L.H., J.H.M. and S.M. characterized the anti-MRSA antibodies. Y.K., H.H., K.M.L., E.P. and J.C. did mass spectrometry analysis of the rifalogues during *in vitro* efficacy studies. P.L. and R.F. performed X-ray crystallography of anti-β-WTA monoclonal antibody. J.P.L. designed the synthesis of β-phospho-ribitol. B.-C.L. and C.C. characterized FRET constructs and helped with video microscopy. E.L. determined the number of antibody-binding sites on MRSA. M.S., K.K. and P.S.A. isolated anti-MRSA antibodies from patients. M.W.T. contributed to bacterial genetics and data analysis. E.J.B. and S.M. initiated the project and S.M. led the project. S.M.L., E.J.B. and S.M. composed the paper with input from all authors.

**Additional Information** The structure of the anti-β-WTA Fab bound to the synthetic WTA fragment (β-GlcNAc anomer) has been deposited in the Protein Data Bank under accession number 5D6C. Reprints and permissions information is available at www.nature.com/reprints. The authors declare competing financial interests: details are available in the online version of the paper. Readers are welcome to comment on the online version of the paper. Correspondence and requests for materials should be addressed to E.J.B. (brown.eric@gene.com) or S.M. (sanj@gene.com).

## METHODS

**Ethics statement.** All animal procedures were conducted under a protocol (#08–1990) approved by the Genentech Institutional Animal Care and Use Committee in an Association for Assessment and Accreditation of Laboratory Animal Care (AAALAC)-accredited facility in accordance with the Guide for the Care and Use of Laboratory Animals and applicable laws and regulations. For cloning of antibodies from human B cells, informed written consent was obtained from all donors and was provided in accordance with the Declaration of Helsinki. Approval was obtained from the health research ethics committee of Denmark through the regional committee for the Capital Region of Denmark.

**Bacterial strains.** All *in vivo* experiments were done with MRSA-USA300 NRS384 obtained from NARSA (https://www.beiresources.org) unless noted otherwise. The generation of protein-A-deficient strain Δ*mcr* USA300 NRS384, as well as protein-A-deficient USA300 lacking *tarM* or *tarS* has been described previously[38,39]. The protein-A-deficient strains were used only in some *in vitro* experiments to determine antibody specificity.

**MIC determinations for extracellular bacteria.** The MIC for extracellular bacteria was determined by preparing serial twofold dilutions of the antibiotic in tryptic soy broth. Dilutions of the antibiotic were made in quadruplicate in 96-well culture dishes. MRSA (NRS384 strain of USA300) was taken from an exponentially growing culture and diluted to $1 \times 10^4$ c.f.u. ml$^{-1}$. The bacteria were cultured in the presence of antibiotic for 18–24 h with shaking at 37 °C and bacterial growth was determined by reading the optical density (OD) at 630 nm. The MIC was determined to be the dose of antibiotic that inhibited bacterial growth by >90%.

**MIC determinations for intracellular bacteria.** Intracellular MIC was determined on bacteria that were sequestered inside mouse peritoneal macrophages (see later for generation of murine peritoneal macrophages). Macrophages were plated at a density of $4 \times 10^5$ cells ml$^{-1}$ and infected with MRSA at a ratio of 10–20 bacteria per macrophage. Macrophage cultures were maintained in growth media supplemented with 50 μg ml$^{-1}$ of gentamycin to inhibit the growth of extracellular bacteria and test antibiotics were added to the growth media 1 day after infection. The survival of intracellular bacteria was assessed 24 h after addition of the antibiotics. Macrophages were lysed with Hanks buffered saline solution supplemented with 0.1% bovine serum albumin (BSA) and 0.1% Triton-X, and serial dilutions of the lysate were made in PBS solution containing 0.05% Tween-20. The number of surviving intracellular bacteria was determined by plating on tryptic soy agar plates with 5% defibrinated sheep blood.

***In vivo* transfer of infection model.** USA300 stocks were prepared for infection from actively growing cultures in tryptic soy broth. Bacteria were washed three times in PBS and aliquots were frozen at −80 °C in PBS 25% glycerol.

*Intracellular bacteria infections.* Seven-week-old female A/J mice (Stock 000646) were obtained from Jackson Labs and infected by peritoneal injection with $5 \times 10^7$ c.f.u. of USA300. Mice were killed 1 day after infection and the peritoneum was flushed with 5 ml of cold PBS. Peritoneal washes were centrifuged for 5 min at 1,000 r.p.m. at 4 °C in a table-top centrifuge. The cell pellet containing peritoneal cells was collected and cells were treated with 50 μg ml$^{-1}$ of lysostaphin (Cell Sciences, CRL 309C) for 20 min at 37 °C to kill contaminating extracellular bacteria. Peritoneal cells were washed three times in ice-cold PBS to remove the lysostaphin. Peritoneal cells from donor mice were pooled, and recipient mice were injected with cells derived from five donors per each recipient by intravenous injection into the tail vein. To determine the number of live intracellular colony-forming units, a sample of the peritoneal cells were lysed in HB (Hanks balanced salt solution supplemented with 10 mM HEPES and 0.1% BSA) with 0.1% Triton-X, and serial dilutions of the lysate were made in PBS with 0.05% Tween-20.

*Free bacteria infections.* A/J mice were infected with various doses of free bacteria using a fresh aliquot of the glycerol stocks used for the peritoneal injections. Actual infection doses were confirmed by c.f.u. plating. For the data shown in Fig. 1a the actual infection dose for intracellular bacteria was $1.8 \times 10^6$ c.f.u. per mouse, and the actual infection dose for free bacteria was $2.9 \times 10^6$ c.f.u. per mouse. Selected mice were treated with a single dose of 110 mg kg$^{-1}$ of vancomycin by intravenous injection immediately after infection.

***In vitro* transfer of infection to non-phagocytic cells.** *Generation of MRSA-infected peritoneal cells.* Six-to-eight-week-old female A/J mice (see earlier) were infected with $1 \times 10^8$ c.f.u. of the NRS384 strain of USA300 by peritoneal injection. The peritoneal wash was harvested 1 day after infection, and the infected peritoneal cells were treated with 50 μg ml$^{-1}$ of lysostaphin diluted in HEPES buffer supplemented with 0.1% BSA (HB buffer) for 20 min at 37 °C. Peritoneal cells were then washed twice in ice-cold HB buffer. The peritoneal cells were diluted to $1 \times 10^6$ cells ml$^{-1}$ in RPMI 1640 tissue culture media supplemented with 10 mM HEPES and 10% fetal calf serum, and 5 μg ml$^{-1}$ vancomycin. Free MRSA from the primary infection was stored overnight at 4 °C in PBS solution as a control for extracellular bacteria that were not subject to neutrophil killing.

*Infection of osteoblasts, HBMEC and A549 cells.* MG63 cell line (CRL-1427) and A549 cells (CCL185) were obtained from ATCC and maintained in RPMI 1640 tissue culture media supplemented with 10 mM HEPES and 10% fetal calf serum (RPMI-10). HBMEC cells (catalogue #1000) and ECM media (catalogue #1001) were obtained from ScienceCell Research Labs. The cells were used without further authentication or testing for mycoplasma contamination. Cells were plated in 24-well tissue culture plates and cultured to obtain a confluent layer. On the day of the experiment, the cells were washed once in RPMI (without supplements). MRSA or infected peritoneal cells were diluted in complete RPMI-10 and vancomycin was added at 5 μg ml$^{-1}$ immediately before infection. Peritoneal cells were added to the osteoblasts at $1 \times 10^6$ peritoneal cells per ml. A sample of the cells was lysed with 0.1% Triton-X to determine the actual concentration of live intracellular bacteria at the time of infection. The actual titre for all infections was determined by plating serial dilutions of the bacteria on tryptic soy agar with 5% defibrinated sheep blood.

**Generation of the anti-*S. aureus* antibodies.** The human IgG antibodies against anti-β-GlcNAc WTA monoclonal antibody (mAb) and anti-α-GlcNAc WTA mAb were cloned from peripheral B cells from patients after *S. aureus* infection using a monoclonal antibody discovery technology that conserves the cognate pairing of antibody heavy and light chains[40]. Antibodies were expressed by transfection of mammalian cells[41]. Supernatants containing full-length IgG1 antibodies were harvested after 7 days and used to screen for antigen binding by enzyme-linked immunosorbent assay (ELISA). These antibodies were positive for binding to cell wall preparations from USA300. Antibodies were subsequently produced in 200-ml transient transfections and purified with protein A chromatography (MabSelect SuRe, GE Life Sciences) for further testing.

**Synthesis of the linker drug.** Synthesis of the rifalogue linker drug was performed as follows. Protease cleavable linker MC-VC-PAB-OH[23] (1.009 g, 1.762 mmol, 1.000, 1,009 mg) was taken up in *N*,*N*-dimethylformamide (6 ml, 77 mmol, 44, 5,700 mg). To this was added a solution of thionyl chloride (1.1 equiv., 1.938 mmol, 1.100, 231 mg) in dichloromethane (DCM) (1 ml, 15.44 mmol, 8.765, 1,325 mg) in portions dropwise (half was added over 1 h, stirred for 1 h at room temperature, then the other half was added over another hour). The solution remained a yellow colour. Another 0.6 equiv. of thionyl chloride was added as a solution in 0.5 ml DCM dropwise, carefully. The reaction remained yellow and was stirred sealed overnight at room temperature. The reaction was monitored by liquid chromatography mass spectrometry (LC/MS), indicating 88% conversion to benzyl chloride. Another 0.22 equiv. of thionyl chloride was added dropwise as a solution in 0.3 ml DCM. When the reaction approached 92% benzyl chloride, the reaction was bubbled with $N_2$. The concentration was increased from 0.3 M to 0.6 M.

MC-VC-PAB-Cl (0.9 mmol) was cooled to 0 °C and rifalogue (dimethyl piperazinebenzoxazinorifamycin[42] (0.75 g, 0.81 mmol, 0.46, 750 mg)) was added. The mixture was diluted with another 1.5 ml of DMF to reach 0.3 M. Stirred open to air for 30 min. *N*,*N*-diisopropylethylamine (3.5 mmol, 3.5 mmol, 2.0, 460 mg) was added and the reaction stirred overnight open to air. Over the course of 4 days, four additions of 0.2 equiv. *N*,*N*-diisopropylethylamine base were added while the reaction stirred open to air, until the reaction appeared to stop progressing. The reaction was diluted with DMF and purified on high-performance liquid chromatography (HPLC; 20–60% ACN/FA·$H_2O$) in several batches to give MC-VC-PAB-rifalogue (0.38 g, 32% yield) $m/z = 1{,}482.8$.

The non-cleavable rifalogue linker drug was synthesized using the exact same method, but replacing MC-VC-PAB-OH with MC-V-D-Cit-PAB-OH.

**Conjugation of the linker drug to antibody.** Construction and production of the THIOMAB variant of anti-WTA antibody was done as reported previously[43]. Briefly, a cysteine residue was engineered at the Val 205 position of the anti-WTA light chain to produce its THIOMAB variant. The thio anti-WTA was conjugated to MC-vc-PAB-rifalogue. The antibody was reduced in the presence of 50-fold molar excess dithiothreitol (DTT) overnight. The reducing agent and the cysteine and glutathione blocks were purified away using HiTrap SP-HP column (GE Healthcare). The antibody was re-oxidized in the presence of 15-fold molar excess dehydroascorbic acid (MP Biomedical) for 2.5 h. The formation of interchain disulfide bonds was monitored by LC/MS. A threefold molar excess of the linker drug (MC-VC-PAB-rifalogue) over protein was incubated with the THIOMAB for 1 h. The AAC was purified by filtration through a 0.2 μm SFCA filter (Millipore). Excess-free linker drug was removed by filtration. The conjugate was buffer exchanged into 20 mM histidine acetate pH 5.5/240 mM sucrose by dialysis. The number of conjugated MC-VC-PAB-rifalogue molecules per mAb was quantified by LC/MS analysis. Purity was also assessed by size-exclusion chromatography.

**Mass spectrometric analysis.** LC/MS analysis was performed on a 6530 Accurate-Mass Quadrupole Time-of-Flight (Q-TOF) LC/MS (Agilent Technologies). Samples were chromatographed on a PRLP-S column, 1,000 Å, 8 µm (50 mm × 2.1 mm, Agilent Technologies) heated to 80 °C. A linear gradient from 30–60% B in 4.3 min (solvent A, 0.05% TFA in water; solvent B, 0.04% TFA in acetonitrile) was used and the eluent was directly ionized using the electrospray source. Data were collected and deconvoluted using the Agilent Mass Hunter qualitative analysis software. Before LC/MS analysis, AAC was treated with lysyl endopeptidase (Wako) for 30 min at 1:100 w/w enzyme to antibody ratio, pH 8.0, and 37 °C to produce the Fab and the Fc portion for ease of analysis. The drug-to-antibody ratio (DAR) was calculated using the abundance of Fab and Fab+1 calculated by the MassHunter software.

**Flow cytometry to compare expression of anti-MRSA antibodies.** *Analysis of bacteria isolated from infected mice.* Balb/c mice were infected with $1 \times 10^7$ c.f.u. of MRSA (USA300) by intravenous injection and kidneys were harvested on day 3 after infection. Kidneys were homogenized using a GentleMACS dissociator in 5 ml volume per two kidneys using M-Tubes and the program RNA01.01 (Miltenyi Biotec). Homogenization buffer was: PBS plus 0.1% Triton-X-100, 10 µg ml$^{-1}$ DNAase (bovine pancreas grade II, Roche) and protease inhibitors (complete protease inhibitor cocktail, Roche 11-836-153001). After homogenization, the samples were incubated at room temperature for 10 min and then diluted with ice-cold PBS and filtered through a 40 µm cell strainer. Tissue homogenates were washed twice in ice-cold PBS and then suspended in a volume of 0.5 ml per two kidneys in HB buffer (Hanks balanced salt solution supplemented with 10 mM HEPES and 0.1% BSA). The cell suspension was filtered again and 25 µl of the bacterial suspension was taken for each staining reaction (Fig. 2c).

*Antibody staining for flow cytometry.* Bacteria ($1 \times 10^7$ of *in vitro* grown bacteria (Fig. 2d), or 25 µl of tissue homogenate described earlier (Fig. 2c) were suspended in HB buffer and blocked by incubation with 400 µg ml$^{-1}$ of mouse IgG (Sigma, I5381) for 1 h. Fluorescently labelled antibodies were added directly to the blocking reaction and incubated at room temperature for an additional 10–20 min. Bacteria were washed three times in HB buffer and then fixed in PBS 2% paraformaldehyde before FACS analysis. Test antibodies (anti-β-WTA, anti-α-WTA or isotype control-anti CMV-gD) were conjugated with Alexa-488 using amine reactive reagents (Invitrogen, succinimidyl-ester of Alexa Fluor 488, NHS-A488). Antibodies in 50 mM sodium phosphate were reacted with a 5–10-fold molar excess of NHS-A488 in the dark for 2–3 h at room temperature. The labelling mixture was applied to a GE Sepharose S200 column equilibrated in PBS to remove excess reactants from the conjugated antibody. The number of A488 molecules per antibody was determined using the ultraviolet method as described by the manufacturer.

For analysis of bacteria in tissue homogenates a non-competing anti-*S. aureus* antibody (rF1 (ref. 38)) was conjugated to Alexa-647 to distinguish *S. aureus* from similar sized particles. Test antibodies were examined at a range of doses from 80 ng ml$^{-1}$ to 50 µg ml$^{-1}$. Flow cytometry was performed using a Beckton Dickson FACS ARIA (BD Biosciences) and analysis was performed using FlowJo analysis software (Flow Jo LLC).

**WTA–antibody complex purification and crystallization.** The anti-β-WTA antibody Fab fragment was expressed in *Escherichia coli* and purified on Protein G Sepharose followed by SP sepharose cation exchange and size-exclusion chromatography. Antibody was concentrated to 30 mg ml$^{-1}$ in MES buffer (20 mM MES pH 5.5, 150 mM NaCl) and mixed with a 2:1 mol/mol ratio of the WTA analogue (diluted in water) for crystallization trials. Sparse matrix crystallization screening provided initial hits in PEG-8000 based conditions, which were further optimized to provide diffraction quality crystals. Ultimately, data were collected on a crystal grown by the vapour diffusion method in a sitting drop containing 0.5 µl protein and 0.5 µl 0.08 M sodium cacodylate pH 6.5, 0.16 M calcium acetate, 14.4% PEG-8000, and 20% glycerol. Crystals were cryo-protected in mother liquor, flash frozen in liquid nitrogen, and stored for data collection at 100 K.

**Data collection and structure determination.** Data were collected to 1.7 Å at beamline 22ID at the Advanced Photon Source (APS) under cryo-cooled conditions (100 K) at a wavelength of 1.0 Å. Data were reduced using HKL2000 and SCALEPACK in the space group $P2_12_12_1$, with unit cell parameters of $a = 63.7$ Å, $b = 111.4$Å, $c = 158.4$ Å (see Extended Data Table 1 for processing statistics). The structure was solved by sequential molecular replacement searches using Fab constant and variable regions (Protein Data Bank accession 4I77) as individual search models. Iterative rounds of manual model adjustment with COOT followed by simulated annealing, coordinate, and *b*-factor refinement with Phenix and BUSTER (Global Phasing) gave a final model with $R/R_{free}$ values of 20.6% and 23.7% respectively. Ramachandran statistics calculated by MolProbity indicate that 97.2% of the model residues lie in favoured regions, with 0.5% outliers.

**Generation of a synthetic WTA fragment.** *Synthesis of dibenzyl phosphorochloridate.* A mixture of NCS (3.5 g, 26.6 mmol) was suspended in toluene (80 ml). Then dibenzyl phosphonate (2.0 g, 7.6 mmol) was added. The mixture was stirred at room temperature overnight. The white solid was filtered off and the organic phase was evaporated to give dibenzyl phosphorochloridate (**1**; 2.1 g, 96%) as light yellow oil. $^1$H NMR (300 MHz, $CDCl_3$, 25 °C) $\delta$ 7.36 (s, 10H), 5.20 (m, 4H).

*Synthesis of 4-O-(2-acetamido-3,4,6-tri-O-acetyl-2-deoxy-β-D-glucopyranosyl)-1-O-acetyl-D-ribitol-5-dibenzylphosphate.* A mixture of **2** (described in ref. 44) (500 mg, 0.95 mmol) dissolved in pyridine (12 ml) was cooled to −30 °C and **1** (described ref. 44) (595 mg, 2.0 mmol) was added, stirring for 2 h at −30 °C and warmed to room temperature for 4 h. The mixture was added to $H_2O$, and concentrated *in vacuo*. The residue was purified by column chromatography (silica gel: 200 to ~300 mesh; dichloromethane: methanol in a 30:1 as eluent) to give 4-*O*-(2-acetamido-3,4,6-tri-*O*-acetyl-2-deoxy-β-D-glucopyranosyl)-1-*O*-acetyl-D-ribitol-5-dibenzylphosphate (**3**; 190 mg, 24%) as light yellow solid. $^1$H NMR (300 MHz, Acetone-$d_6$, 25 °C) $\delta$ 7.29–7.23 (m, 10H), 7.08 (d, 1H), 5.08 (t, 1H), 4.99–4.78 (m, 6H), 4.31–3.97 (m, 8H), 3.82–3.63 (m, 3H), 1.88 (s, 3H), 1.86 (s, 6H), 1.79 (s, 3H), 1.69 (s, 3H). LC/MS (*m*/*z*) ES+ 784 $[M+H]^+$.

*Synthesis of 4-O-(2-acetamido-3,4,6-tri-O-acetyl-2-deoxy-β-D-glucopyranosyl)-1-O-acetyl-D-ribitol-5-phosphate.* A mixture of **3** (150 mg, 0.19 mmol) dissolved in MeOH (6 ml) was hydrogenated over 10% Pd/C (20 mg) for 2 h at room temperature. Then the mixture was filtered, and the filtrate was evaporated to give 4-*O*-(2-acetamido-3,4,6-tri-*O*-acetyl-2-deoxy-β-D-glucopyranosyl)-1-*O*-acetyl-D-ribitol-5-phosphate (**4**; 100 mg) as light yellow oil. LC/MS (*m*/*z*) ES+ 604 $[M+H]^+$.

*Synthesis of 4-O-(2-acetamido-2-deoxy-β-D-glucopyranosyl)-D-ribitol-5-phosphate (**5**).* A mixture of **4** (80 mg, 0.16 mmol) dissolved in MeOH (10 ml) was cooled to 5 °C and $K_2CO_3$ (30 mg, 0.21 mmol) was added and stirred at 5 °C for 3 h. The reaction was then quenched with 1 N HCl, and concentrated *in vacuo*. The crude product was purified by gel filtration (LH-20, MeOH) to give 4-*O*-(2-acetamido-2-deoxy-β-D-glucopyranosyl)-D-ribitol-5-phosphate (**5**; 13.3 mg, 23%) as a white solid $^1$H NMR (300 MHz, MeOH-$d_4$, 25 °C) $\delta$ 4.62 (d, 1H), 4.30–4.02 (m, 3H), 3.92–3.32 (m, 9H), 2.03 (s, 3H). LC/MS (*m*/*z*) ES+ 436 $[M+H]^+$.

**Time of kill for free antibiotics on non-replicating bacteria.** *S. aureus* (USA300) was taken from an overnight stationary phase culture, washed once in PBS and suspended at $1 \times 10^7$ c.f.u. ml$^{-1}$ in PBS with no antibiotic or with $1 \times 10^{-6}$ M antibiotic in a 10 ml volume in 50 ml polypropylene centrifuge tubes. The bacteria were incubated at 37 °C overnight with shaking. At each time point, three 1 ml samples were removed from each culture and centrifuged to collect the bacteria. Bacteria were washed once with PBS to remove the antibiotic and the total number of surviving bacteria was determined by plating serial dilutions of the bacteria on agar plates.

**Killing of persister cells by free antibiotics.** *S. aureus* (USA300) was taken from an overnight stationary phase culture, washed once in tryptic soy broth (TSB) and then adjusted to a final concentration of $1 \times 10^7$ c.f.u. ml$^{-1}$ in a total volume of 10 ml of either TSB or TSB with ciprofloxicin (0.05 mM). Cultures were incubated with shaking at 37 °C for 6 h and then the second antibiotic, either rifampicin (1 µg ml$^{-1}$) or the rifalogue (1 µg ml$^{-1}$) was added. At the indicated times, samples were removed from each culture, washed once with PBS to remove the antibiotic and re-suspended in PBS. The total number of surviving bacteria was determined by plating serial dilutions of the bacteria on agar plates. At the final time point the remainder of each culture was collected and plated.

**Cathepsin release assay for AAC.** To quantify the amount of active antibiotic released from AACs after treatment with cathepsin B, AACs were diluted to 200 µg ml$^{-1}$ in cathepsin buffer (20 mM sodium acetate, 1 mM EDTA, 5 mM L-cysteine, pH 5). Cathepsin-B (from bovine spleen, Sigma C7800) was added at 10 µg ml$^{-1}$ and the samples were incubated for 1 h at 37 °C. As a control, AACs were incubated in buffer alone. The reaction was stopped by addition of 9 volumes of bacterial growth media, TSB pH 7.4. To estimate the total release of active antibiotic, serial dilutions of the reaction mixture were made in quadruplicate in TSB in 96-well plates and MRSA (USA300) was added to each well at a final density of $2 \times 10^3$ c.f.u. ml$^{-1}$. The cultures were incubated overnight at 37 °C with shaking and bacterial growth was measured by reading absorbance at 630 nM using a plate reader.

**Synthesis of anti-β-WTA antibody FRET conjugate.** We synthesized and conjugated a maleimide FRET peptide to the anti-β-WTA THIOMAB antibody. We used a FRET pair of tetramethylrhodamine (TAMRA) and fluorescein. The maleimide FRET peptide was synthesized by standard Fmoc solid-phase chemistry using a PS3 peptide synthesizer (Protein Technologies; B.-C.L., M.D. and R.V., manuscript in preparation)[27]. Briefly, 0.1 mmol of Rink amide resin was used to generate C-terminal carboxamide. We used a Fmoc-Lys(Mtt)-OH at the N- and C-terminal residues in order to remove the Mtt group on the resin and carry out additional

side-chain chemistry to attach TAMRA and fluorescein. The sequence of Val-Cit-Leu was added between the FRET pair as a cathepsin-cleavable spacer. The crude maleimide FRET peptide or maleimidocarproyl-K(TAMRA)-G-V-Cit-L-K (fluorescein) cleaved off from the resin was subjected to further purification by reverse-phase HPLC with a Jupiter 5u C4 column (5 μm, 10 mm × 250 mm; Phenomenex). Our FRET probe allows monitoring not only of the intracelluar trafficking of the antibody conjugate, but also the processing of the linker in the phagolysosome. The intact antibody conjugate fluoresces only in red due to the fluorescence resonance energy transfer from the donor. However, upon the substrate cleavage of the FRET peptide in the phagolysosome, the green fluorescence from the donor is expected to appear.

**Video microscopy to detect cleavage of the linker inside macrophages.** Murine peritoneal macrophages were plated on chamber slides (Ibidi, catalogue 80826) in complete media as described for the macrophage intracellular killing assay. USA300 was labelled with Cell Tracker Violet (Invitrogen C10094) at 100 μg ml$^{-1}$ in PBS 0.1% BSA by incubation for 30 min at 37 °C. The labelled bacteria were opsonized with the anti-β-WTA-FRET probe by incubation for 1 h in HB buffer. Macrophages were washed once immediately before addition of the opsonized bacteria, and bacteria were added to cells at $1 \times 10^7$ bacteria per ml. For no-phagocytosis controls, the macrophages were pre-treated with 60 nM Latrunculin A (Calbiochem) for 30 min before and during phagocytosis. The slides were placed on the microscope immediately after addition of bacteria to the cells and movies were acquired with a Leica SP5 confocal microscope equipped with an environmental chamber with $CO_2$ and temperature controllers from Ludin. The images were captured every minute for a total time of 30 min using a Plan APO CS ×40, N.A: 1.25, oil immersion lens, and the 488 nm and 543 nm laser lines to excite Alexa-488 and TAMRA, respectively. Phase images were also recorded using the 543 nm laser line.

**Quantification of released antibiotic inside macrophages.** Primary murine peritoneal macrophages or RAW 264.7 cells (purchased from ATCC) were infected in 24-well tissue culture dishes as described later for the intracellular killing assay with MRSA opsonized with AAC at 100 μg ml$^{-1}$ in HB. The RAW 264.7 cells were used without further authentication or testing for mycoplasma contamination. After phagocytosis was complete, the cells were washed and 250 μl of complete media plus gentamycin was added to wells and the cells were incubated for the indicated time points. At each time point, the supernatant and cellular fractions were collected followed by acetonitrile (ACN) addition to 75% final concentration and incubated for 30 min. Cell and supernatant extracts were lyophilized by evaporation under N2 (TurboVap; Biotage) and reconstituted in 100 μl of 50% ACN, filtered using a 0.45 glass fibre filter plate (Phenomenex) and analysed by LC/MS/MS as follows.

The rifalogue was separated on an Acquity UPLC (Waters Corporation) under gradient elution using a Phenomenex Kinetex XB-C18 column (100 Å, 50 × 2.1 mm internal diameter, 2.6 μm particle size). The column was maintained at room temperature. The mobile phase was a mixture of 10 mM ammonium acetate in water containing 0.1% formic acid (A) and 90% acetonitrile (B) at a flow rate of 1 ml min$^{-1}$. The rifalogue was eluted with a gradient of 3–98% B over 1 min, followed by 0.8 min at 98% B, then 0.7 min of 3% B to re-equilibrate the column. The injection volume was 10 μl.

The Triple Quad 6500 mass spectrometer (Ab Sciex) was operated in a positive ion multiple reaction-monitoring (MRM) mode. The rifalogue precursor (Q1) ion monitored was 927.6 *m*/*z* and the product (Q3) ion monitored was 895.2 *m*/*z* with collision energy at 27 eV and declustering potential at 191 V. The MS/MS setting parameters were as follows: ion spray voltage, 5,500 V; curtain gas, 40 psi; nebulizer gas (GS1), 35 psi, (GS2), 50 psi; temperature, 600 °C; and dwell time, 150 ms.

Linear calibration curves were obtained for 0.41–100 nM concentration range by spiking rifalogue into cell or supernatant fractions (lacking MRSA or AAC) that were treated similarly to samples. Concentrations of rifalogue were calculated with MultiQuant software (Ab Sciex).

***In vitro* intracellular killing assay.** *Non-phagocytic cell types.* MG63 (CRL-1427) and A549 (CCL185) cell lines were obtained from ATCC and maintained in RPMI 1640 tissue culture media supplemented with 10 mM HEPES and 10% fetal calf serum (RPMI-10). HUVEC cells were obtained from Lonza and maintained in EGM endothelial cell complete media (Lonza). HBMEC cells (catalogue #1000) and ECM media (catalogue #1001) were obtained from ScienceCell Research Labs. The cells were used without further authentication or testing for mycoplasma contamination.

*Murine macrophages.* Peritoneal macrophages were isolated from the peritoneum of 6–8-week-old Balb/c mice (Charles River Laboratories). To increase the yield of macrophages, mice were pre-treated by intraperitoneal injection with 1 ml of thioglycolate media (Becton Dickinson). The thioglycolate media was prepared at a concentration of 4% in water, sterilized by autoclaving, and aged for 20 days to 6 months before use. Peritoneal macrophages were harvested 4 days after treatment with thioglycolate by washing the peritoneal cavity with cold PBS. Macrophages were plated in DMEM supplemented with 10% fetal calf serum, and 10 mM HEPES, without antibiotics, at a density of $4 \times 10^5$ cells well$^{-1}$ in 24-well culture dishes. Macrophages were cultured overnight to permit adherence to the plate.

*Human M2 macrophages.* CD14$^+$ monocytes were purified from normal human blood using a Monocyte Isolation Kit II (Miltenyi, catalogue 130-091-153) and plated at $1.5 \times 10^5$ cells cm$^{-2}$ on tissue culture dishes pre-coated with fetal calf serum (FCS) and cultured in RPMI 1640 media with 20% FCS plus 100 ng ml$^{-1}$ rhM-CSF. Media was refreshed on day 1 and on day 7, the media was changed to 5% serum plus 20 ng ml$^{-1}$ IL-4. Macrophages were used 18 h later.

*Assay protocol.* In all experiments bacteria were cultured in TSB. To assess intracellular killing with AACs, USA300 was taken from an exponentially growing culture and washed in HB. AACs or antibodies were diluted in HB (Hanks balanced salt solution supplemented with 10 mM HEPES and 0.1% BSA) and incubated with the bacteria for 1 h to permit antibody binding to the bacteria (opsonization), and the opsonized bacteria were used to infect macrophages at a ratio of 10–20 bacteria per macrophage ($4 \times 10^6$ bacteria in 250 μl of HB per well). Macrophages were pre-washed with serum-free DMEM media immediately before infection, and infected by incubation at 37 °C in a humidified tissue culture incubator with 5% $CO_2$ to permit phagocytosis of the bacteria. After 2 h, the infection mix was removed and replaced with normal growth media (DMEM supplemented with 10% FCS, 10 mM HEPES) and gentamycin was added at 50 μg ml$^{-1}$ to prevent growth of extracellular bacteria[45]. At the end of the incubation period, the macrophages were washed with serum-free media, and the cells were lysed in HB supplemented with 0.1% Triton-X (lyses the macrophages without damaging the intracellular bacteria). Serial dilutions of the lysate were made in PBS solution supplemented with 0.05% Tween-20 (to disrupt aggregates of bacteria) and the total number of surviving intracellular bacteria was determined by plating on tryptic soy agar with 5% defibrinated sheep blood.

**ELISA for quantification of anti-MRSA antibodies in human serum.** Cell wall preparations (CWPs) were generated from protein-A-deficient *S. aureus* by incubating 40 mg of pelleted bacteria per ml of 10 mM Tris-HCl (pH 7.4) supplemented with 30% raffinose, 100 μg ml$^{-1}$ of lysostaphin (Cell Sciences), and EDTA-free protease inhibitor cocktail (Roche), for 30 min at 37 °C. The lysates were centrifuged at 11,600*g* for 5 min, and the supernatants containing cell wall components were collected.

ELISA experiments were performed using standard protocols. Briefly, plates were pre-coated with CWP and then incubated with human IgG preparations: purified human IGIV Immune Globulin (ASD Healthcare), pooled serum from healthy donors or from MRSA patients. The concentrations of anti-staphylococcal IgG present in the serum or purified IgG were calculated by using a calibration curve that was generated with known concentrations of anti-peptidoglycan mAb (4479) against peptidoglycan.

**Intravenous infection model for testing efficacy of the AAC.** Seven-week-old female mice, Balb/c, were obtained from Jackson West, or SCID mice were obtained from Charles River Laboratories. Infections were carried out by intravenous injection into the tail vein. SCID-huIgG model: CB17.SCID mice were reconstituted with IGIV Immune Globulin (ASD Healthcare) using a dosing regimen optimized to achieve constant serum levels of >10 mg ml$^{-1}$ of human IgG. IGIV was administered with an initial intravenous dose of 30 mg per mouse followed by a second dose of 15 mg per mouse by intraperitoneal injection after 6 h, and subsequent daily dosings of 15 mg per mouse by intraperitoneal injection for 3 consecutive days. Mice were infected 4 h after the first dose of IGIV with $2 \times 10^7$ c.f.u. of MRSA diluted in PBS by intravenous injection. The wild-type USA300, protein-A-sufficient strain was used for all *in vivo* experiments. Mice that received vancomycin were treated with twice daily intraperitoneal injections of 110 mg kg$^{-1}$ of vancomycin starting between 6 and 24 h after infection for the duration of the study. Experimental therapeutics (AAC, anti-MRSA antibodies or free rifalogue antibiotic) were diluted in PBS and administered with a single intravenous injection 30 min to 24 h after infection. All mice were killed on day 4 after infection, and kidneys were harvested in 5 ml of PBS. The tissue samples were homogenized using a GentleMACS dissociator (Miltenyi Biotec). The total number of bacteria recovered per mouse (two kidneys) was determined by plating serial dilutions of the tissue homogenate in PBS 0.05% Tween on tryptic soy agar with 5% defibrinated sheep blood.

**Statistical analysis.** All experiments were performed on biological replicates. Sample size for each experimental group per condition is reported in appropriate figure legends and Methods. For cell culture experiments, sample size was not predetermined, and all samples were included in the analysis. In animal experiments no statistical methods were used to predetermine sample size ($n$ = number

of mice per group), and all animals were used for analysis unless the mice died or had to be euthanized when found moribund. These cases are annotated in the figures. The mice were not randomized after infection, and the investigators were not blinded to outcome assessment. When appropriate, statistically significant differences between control and experimental groups were determined using Mann–Whitney tests.


38. Hazenbos, W. L. *et al.* Novel staphylococcal glycosyltransferases SdgA and SdgB mediate immunogenicity and protection of virulence-associated cell wall proteins. *PLoS Pathog.* **9,** e1003653 (2013).
39. Monk, I. R., Shah, I. M., Xu, M., Tan, M. W. & Foster, T. J. Transforming the untransformable: application of direct transformation to manipulate genetically *Staphylococcus aureus* and *Staphylococcus epidermidis*. *MBio* **3,** e00277–11 (2012).
40. Meijer, P. J. *et al.* Isolation of human antibody repertoires with preservation of the natural heavy and light chain pairing. *J. Mol. Biol.* **358,** 764–772 (2006).
41. Meijer, P. J., Nielsen, L. S., Lantto, J. & Jensen, A. Human antibody repertoires. *Methods Mol. Biol.* **525,** 261–277 (2009).
42. Van Duzer, J. *et al. Rifamycin Analogs and Uses Thereof* (Activbiotics, 2005).
43. Junutula, J. R. *et al.* Site-specific conjugation of a cytotoxic drug to an antibody improves the therapeutic index. *Nature Biotechnol.* **26,** 925–932 (2008).
44. Boullanger, P., Descotes, G., Flandrois, J. P. & Marmet, D. Synthesis of 4-*O*-(2-acetamido-2-deoxy-β-D-glucopyranosyl)-D-ribitol, antigenic determinant of *Staphylococcus aureus*. *Carbohydr. Res.* **110,** 153–158 (1982).
45. Vaudaux, P. & Waldvogel, F. A. Gentamicin antibacterial activity in the presence of human polymorphonuclear leukocytes. *Antimicrob. Agents Chemother.* **16,** 743–749 (1979).

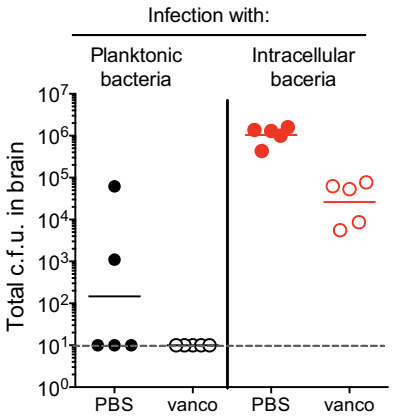


**Extended Data Figure 1 | Intracellular MRSA can infect the brain even in the presence of vancomycin.** *In vivo* infection of mice shown in Fig. 1a. Mice ($n = 5$) were infected with equivalent doses of free bacteria or intracellular bacteria and treated with vancomycin at 110 mg $kg^{-1}$ 10 min after infection and then once per day. Bacterial burden was monitored in the brain 4 days after infection. Bars show geometric mean.

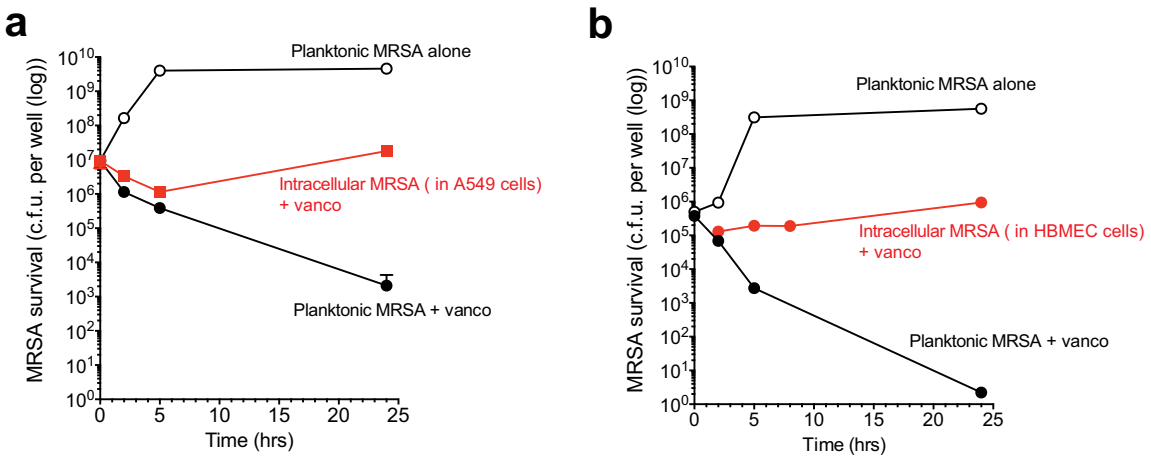


**Extended Data Figure 2 | MRSA is able to grow in the presence of vancomycin when cultured on a monolayer of infectable cells.** **a**, **b**, Similar to the set up in Fig. 1d, planktonic MRSA were either seeded in media alone, or in the presence of vancomycin. Intracellular bacteria were generated by infecting a monolayer of either A549 bronchial epithelial cells (**a**) or HBMECs (**b**) in the presence of vancomycin (vanco). In these experiments plates were centrifuged to promote contact of the bacteria with the monolayer to enhance intracellular infection. At each time point, the culture supernatant was collected to recover extracellular bacteria and adherent cells were lysed to release intracellular bacteria. Extracellular bacteria (planktonic bacteria) grew well in media alone, but were killed by vancomycin. In wells containing a monolayer of mammalian cells (intracellular MRSA + vanco) a fraction of the bacteria were protected from vancomycin during the first 5 h after infection and were able to expand within the intracellular compartment over 24 h. Error bars show s.d. from triplicate wells. Representative of three independent experiments.

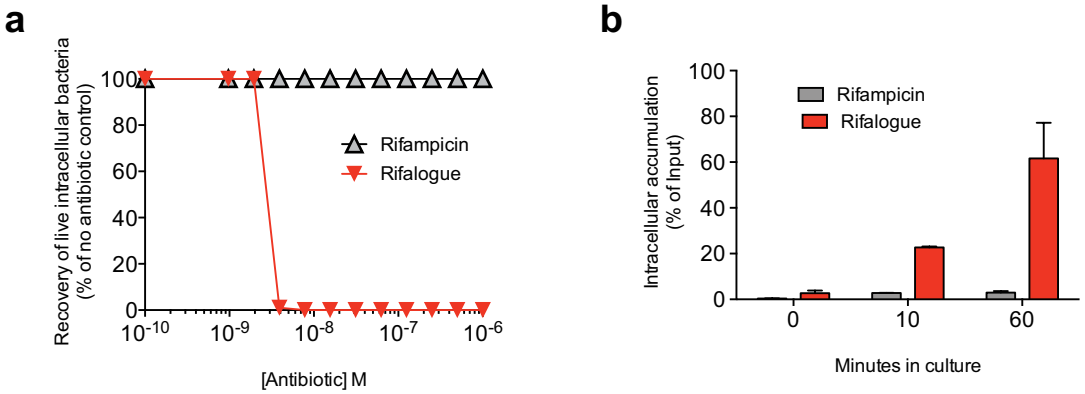


**Extended Data Figure 3 | Rifalogue can also kill intracellular bacteria.** **a**, Determining the intracellular MIC for rifalogue and rifampicin. MRSA was allowed to infect peritoneal macrophages and macrophages were cultured overnight in gentamycin to kill extracellular bacteria. Various doses of rifalogue (red) or rifampicin (grey) were added to the culture medium 1 day after infection and the number of viable intracellular bacteria was determined 24 h later by spotting macrophage lysates onto agar plates. Data shown are representative of more than three independent experiments. **b**, Diffusion of rifalogue versus rifampicin into murine macrophages. Murine peritoneal macrophages were incubated with rifalogue or rifampicin in the culture media. Wells were harvested at 10 and 60 min and the total amount of antibiotic associated with the cells was determined by quantitative mass spectrometry. Results are shown as percentage of input. Error bars show s.d. from triplicate wells. Representative of two experiments. Rifalogue is more lipophilic than rifampicin as a result of its two additional fused aromatic rings, determined by measuring logDs at pH 7, with rifalogue at 3.4, being 100-fold higher than rifampicin (logD 1.3). Additionally, rifalogue has a more basic amine (p$K_a$ 9.7) compared to that found in rifampicin (p$K_a$ 8.2). This balance of lipophilicity and basicity in rifalogue allows it to localize preferentially in lysosomes. It is challenging to develop antibiotics with these properties for systemic administration due to poor pharmacokinetic (PK) properties and toxicity profiles associated with indiscriminate accumulation of these molecules in all host cells. However, appending such antibiotics to an anti-MRSA specific antibody both extends its half-life in the circulation and converts it into an inactive pro-drug whose properties are manifest only after it has been released in phagolysosomes of cells infected with MRSA.

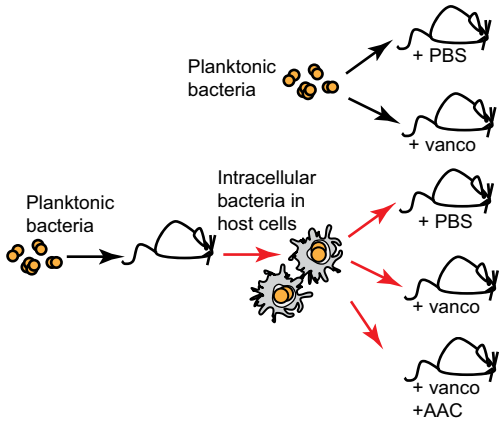


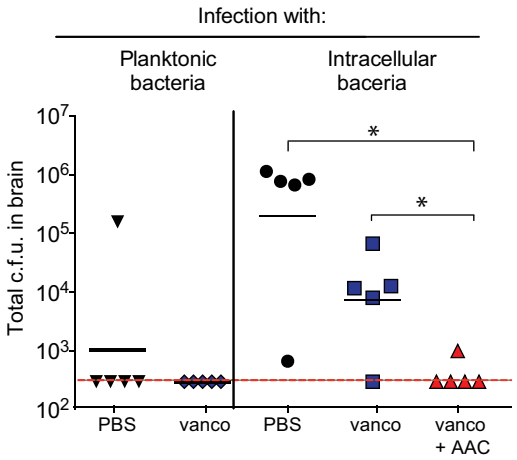


**Extended Data Figure 4 | AAC kills MRSA that survive treatment with vancomycin.** *In vivo* infection of mice as shown in Fig. 1a. Mice were infected with equivalent doses of free bacteria or intracellular bacteria and treated with either saline (PBS) or vancomycin (vanco) at 110 mg $kg^{-1}$, 10 min after infection and then once per day. Selected mice were given vancomycin as described earlier and also treated with a single dose of AAC at 50 mg $kg^{-1}$ 10 min after infection. Four days after infection, bacterial burden was monitored in the brain. Each point represents data from a single mouse ($n = 5$). Bars show geometric mean. *$P < 0.05$, Mann–Whitney *U*-test.

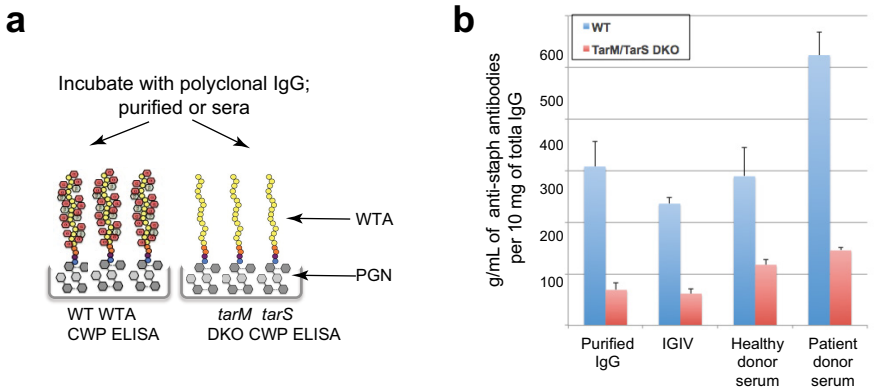


**Extended Data Figure 5 | Human serum contains high levels of anti-*S. aureus* antibodies that can compete with the AAC for binding.** **a**, To estimate the concentration of antibodies that could potentially compete for binding with the anti-β-WTA antibody used in the AAC, human IgG from various sources (normal human serum, serum from MRSA infected patients, purified human IgG (Sigma) or IGIV derived from pooled normal donors) was tested for binding to various bacterial cell wall preparations (CWPs) by enzyme-linked immunosorbent assay (ELISA). CWPs were made from either USA300 (wild type (WT)) or Δ*tarM*Δ*tarS* (DKO) USA300; the latter strain is deficient in the WTA-GlcNAc antigen recognized by the anti-WTA antibodies. For these studies protein-A-deficient USA300 background strains were used to minimize non-specific antibody binding. A standard curve was generated by titrating known amounts of an anti-MRSA antibody directed against peptidoglycan on both cell wall extracts. **b**, Estimated concentration of anti-*S. aureus* antibodies in human serum. The amount of anti-MRSA antibodies in each sample was estimated by comparing the signal obtained for each sample with the standard curve. In the absence of WTA GlcNAc antigens, ~60–70% less serum IgG binding was observed (DKO ELISA; red bars). This indicates the high prevalence of natural antibodies against WTA in adult human serum. Results are reported as μg $ml^{-1}$ of antibody per 10 mg $ml^{-1}$ of total IgG. Error bars show mean ± s.d. from triplicate wells. Data are representative of two independent experiments.

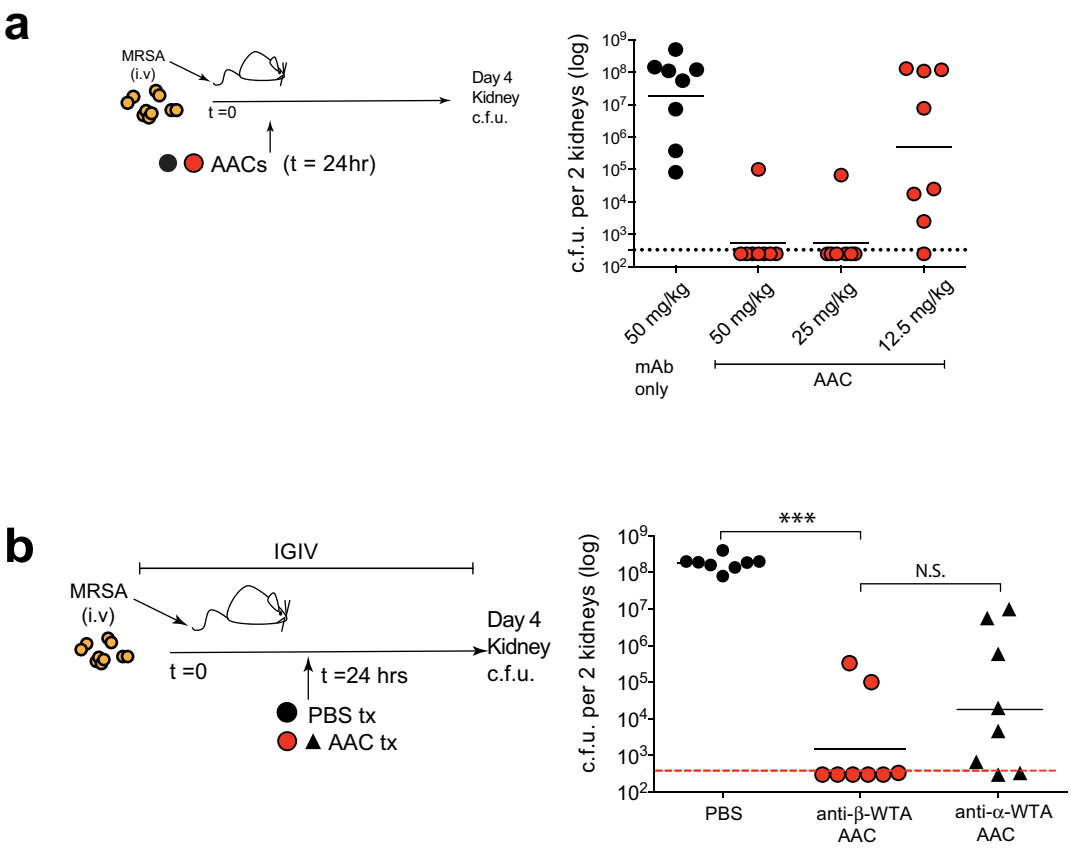


**Extended Data Figure 6 | Optimization of the *in vivo* model of bacteraemia. a**, Titration of AAC in intravenous infection model shown in Fig. 4c ($n = 8$ mice per group). **b**, Efficacy of AACs specific for β-WTA or α-WTA in SCID-IGIV model. SCID mice ($n = 8$ mice per group) were reconstituted with IGIV Immune Globulin using a dosing regimen optimized to achieve constant serum levels of $>10$ mg ml$^{-1}$ of human IgG and infected with MRSA. Mice were treated with 60 mg kg$^{-1}$ of the indicated AACs in a single intravenous injection 1 day after infection and bacterial burden was monitored in kidneys 4 days after infection. Each point represents data from a single animal. Bars show geometric mean. Mann–Whitney test: $***P < 0.005$, not significant (NS) $P > 0.05$.

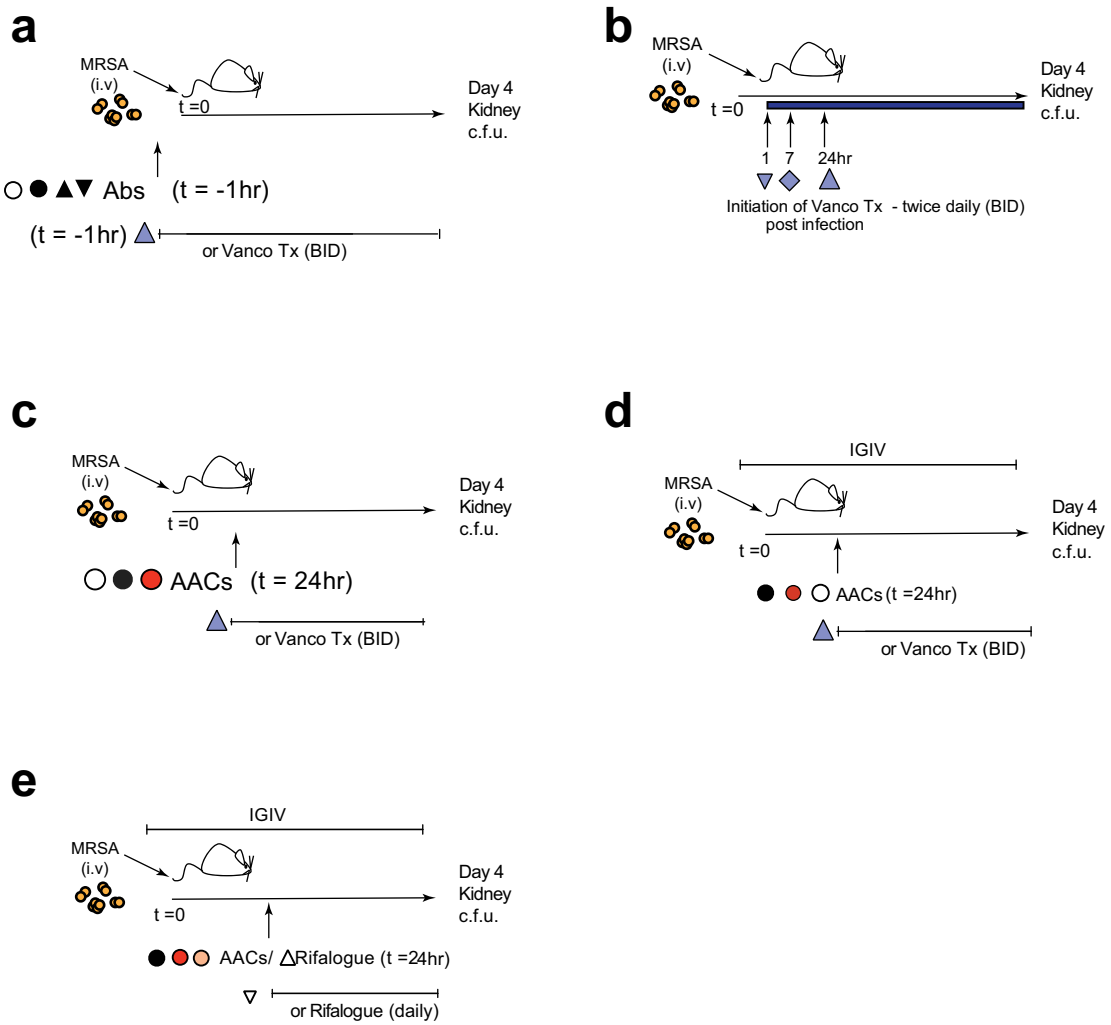


**Extended Data Figure 7 | Schematic of *in vivo* experiments presented in Fig. 4.**

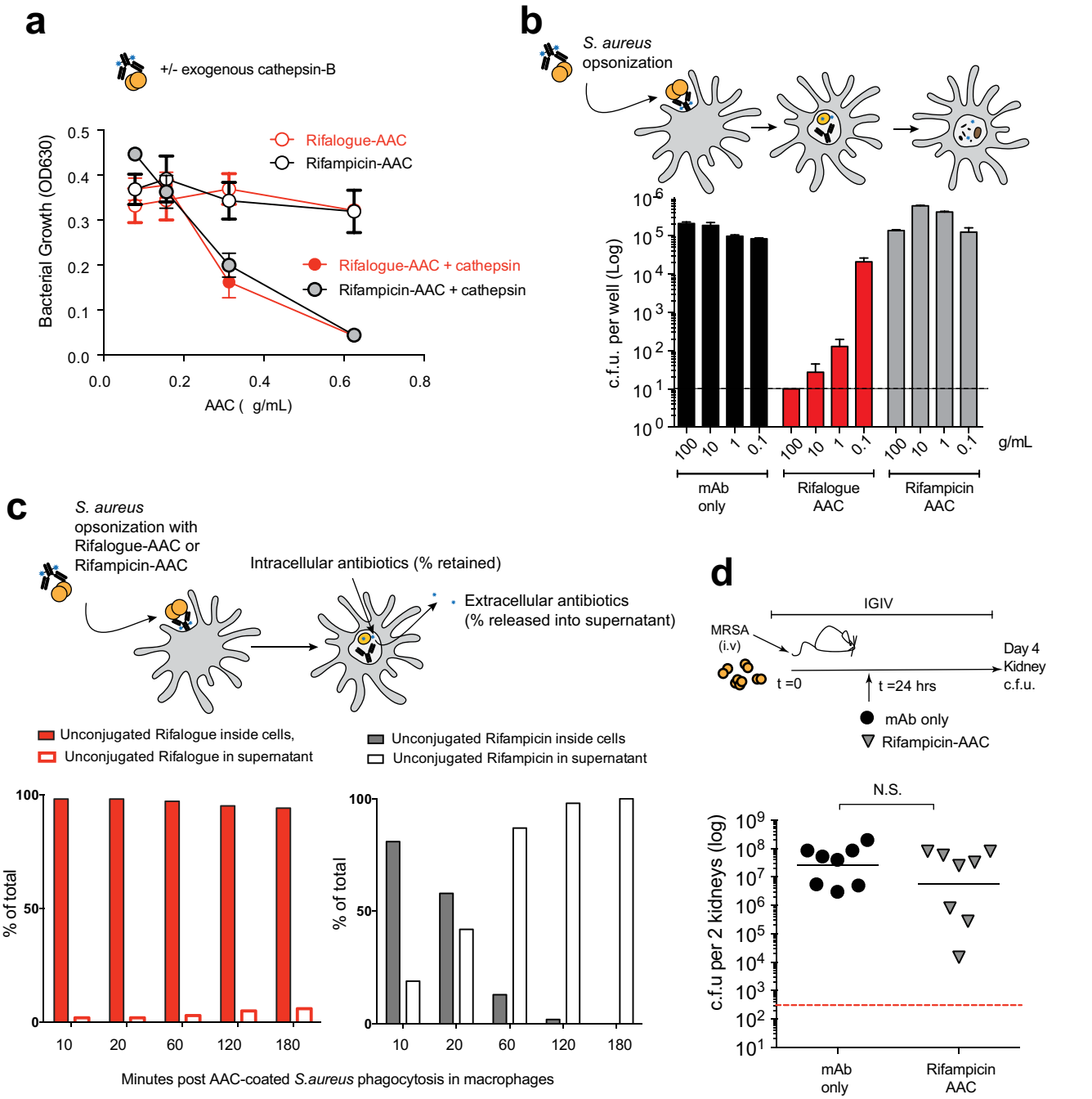


**Extended Data Figure 8 | Comparison of anti-β-WTA AACs made with rifalogue and rifampicin. a**, Rifampicin–AAC and rifalogue–AAC release equivalent amounts of free antibiotic after treatment with exogenous cathepsin-B. Released antibiotics from AACs made with rifalogue (red) and rifampicin (grey) are equally active as they can kill USA300 grown in broth culture. Error bars show s.d. from triplicate wells. **b**, Intracellular killing assay in primary mouse macrophages as shown in Fig. 3c indicates that the rifalogue–AAC, but not rifampicin–AAC is able to kill intracellular *S. aureus*. Error bars show s.d. from triplicate wells. **c**, Greater intracellular retention of unconjugated rifalogue compared with rifampicin after release from AAC inside macrophage cells. MRSA was opsonized with AACs and incubated with macrophages (RAW 264.7 cells) to permit phagocytosis. The macrophages were washed to remove extracellular bacteria and samples of cell lysates or supernatants were collected in triplicate at indicated time points and the total amount of released antibiotic was determined by quantitative mass spectrometry. Error bars represent means ± s.d. from triplicate wells. **a**–**c**, Representative of two or more independent experiments. **d**, Rifampicin–AAC is not efficacious in the SCID-IGIV intravenous infection model as shown in Fig. 4d. Each point represents data from a single mouse ($n = 8$ mice per group). Bars show geometric mean. Mann–Whitney *U*-test: not significant (NS), $P > 0.05$.

**Extended Data Table 1 | Data collection and refinement statistics for anti-β-WTA–WTA complex**

| | anti-βWTA Fab–WTA complex |
|---|---|
| **Data collection** | APS SER-CAT 22ID |
| Space group | $P2_12_12_1$ |
| Cell dimensions | |
| *a*, *b*, *c* (Å) | 63.71, 111.47, 158.41 |
| α, β, γ (°) | 90, 90, 90 |
| Resolution (Å) | 50-1.72 (1.78-1.72) |
| $R_{sym}$ or $R_{merge}$ | 0.056 (0.839) |
| $I / \sigma I$ | 29.4 (2.2) |
| Completeness (%) | 99.9 (99.9) |
| Redundancy | 6.0 (5.9) |
| | |
| **Refinement** | |
| Resolution (Å) | 33.64-1.72 |
| No. reflections (total/test) | 120147/6101 |
| $R_{work}$ / $R_{free}$ | 20.6/23.7% |
| No. atoms | |
| Protein | 6695 |
| WTA | 56 |
| Glycerol | 12 |
| Calcium | 4 |
| Water | 694 |
| *B*-factors | |
| Protein | 35.9 |
| WTA | 56.4 |
| Glycerol | 49.4 |
| Calcium | 38.7 |
| Water | 43.3 |
| R.m.s. deviations | |
| Bond lengths (Å) | 0.010 |
| Bond angles (°) | 1.13 |

*Values in parentheses are for highest-resolution shell.